การจำลองทางคณิตศาสตร์ของเครื่องปฏิกรณ์เคมีแบบเพอร์แวบพอเรชันเมมเบรน
สำหรับเปรียบเทียบสมรรถนะระหว่างการดำเนินงานแบบถังกวนต่อเนื่องกับแบบ
ท่อไหลสำหรับปฏิกิริยาการสังเคราะห์เอสเทอร์

นายจิตรการุณ พงศ์พัฒนพาณิชย์
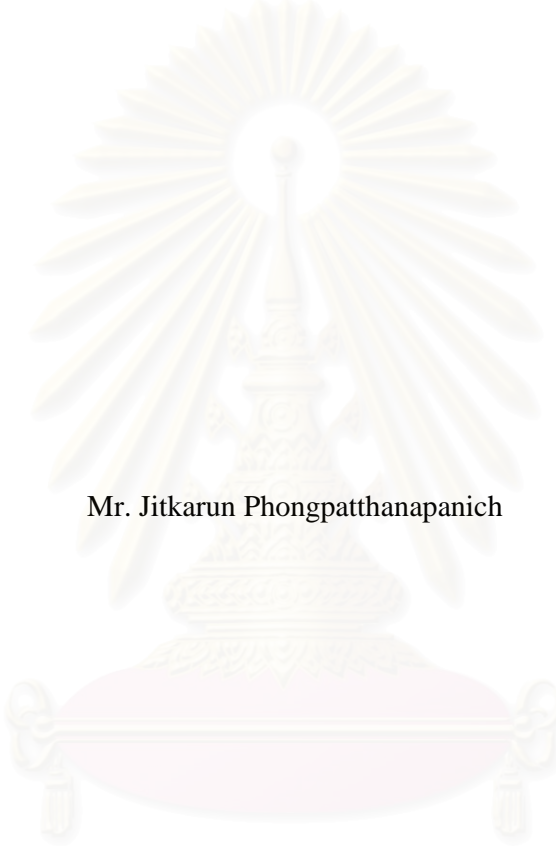
MATHEMATICAL MODELING OF PERVAPORATION MEMBRANE REACTOR FOR COMPARISON OF THE PERFORMANCES BETWEEN CONTINUOUSLY-STIRRED AND PLUG FLOW MODES FOR ESTERIFICATION REACTIONS

Mr. Jitkarun Phongpatthanapanich

Thesis Title	MATHEMATICAL MODELING OF PERVAPORATION MEMBRANE REACTOR FOR COMPARISON OF THE PERFORMANCES BETWEEN CONTINUOUSLY STIRRED AND PLUG FLOW MODES FOR ESTERIFICATION REACTIONS
By	Mr. Jitkarun Phongpatthanapanich
Field of Study	Chemical Engineering
Thesis Advisor	Associate Professor Suttichai Assabumrungrat, Ph.D.

Accepted by the Faculty of Engineering, Chulalongkorn University in Partial Fulfillment of the Requirements for the Master's Degree

….………..…………… Dean of Faculty of Engineering

(Professor Somsak Panyakeow, D.Eng.)

THESIS COMMITTEE

……………………………… Chairman

(Associate Professor Tharathon Mongkhonsi, Ph.D.)

………………………………. Thesis Advisor

(Associate Professor Suttichai Assabumrungrat, Ph.D.)

………………………………. Member

(Assistant Professor Siriporn Damrongsukkul, Ph.D.)

………………………………. Member

(Joongjai Panpranot, Ph.D.)

จิตรการุณ พงศ์พัฒนพาณิชย์: แบบจำลองทางคณิตศาสตร์ของเครื่องปฏิกรณ์เคมีแบบเพอร์แวบพอเรชันเมมเบรนสำหรับเปรียบเทียบสมรรถนะระหว่างการดำเนินงานแบบถังกวนต่อเนื่องกับแบบท่อไหลสำหรับปฏิกิริยาการสังเคราะห์เอสเทอร์ (MATHEMATICAL MODELING OF PERVAPORATION MEMBRANE REACTOR FOR COMPARISON OF THE PERFORMANCES BETWEEN CONTINUOUSLY-STIRRED AND PLUG FLOW MODES FOR ESTERIFICATION REACTIONS)

อ. ที่ปรึกษา: รองศาสตราจารย์ ดร. สุทธิชัย อัสสะบำรุงรัตน์, 91 หน้า. ISBN 974-17-3740-8

วิทยานิพนธ์นี้ศึกษาเปรียบเทียบสมรรถนะของเครื่องปฏิกรณ์แบบเพอร์แวบพอเรชันเมมเบรนที่ดำเนินงานแบบต่าง ๆ สำหรับการสังเคราะห์เมทธิลอะซิเตต (methyl acetate) จากเมทธานอล (methanol) และกรดอะซิติก (acetic acid) โดยสร้างสมการทางคณิตศาสตร์สำหรับศึกษาการดำเนินงานของเครื่องปฏิกรณ์ชนิดนี้ขึ้นมา 3 แบบคือ แบบกึ่งกะ (semi-batch: SB-PVMR) แบบถังกวนต่อเนื่อง (continuous stirred tank: CS-PVMR) และแบบท่อไหล (plug-flow: PF-PVMR) สมการทางคณิตศาสตร์ที่สร้างขึ้นใช้ค่าคงที่ต่าง ๆ ของปฏิกิริยาที่ใช้ตัวเร่งปฏิกิริยาชนิดแอมเบอร์ลิส-15 (Amberlyst-15) และค่าการผ่าน (permeation) ของสารผ่านเมมเรนชนิดโพลิไวนิลแอลกอฮอล์ (PVA) สมการทางคณิตศาสตร์ของปฏิกิริยาและค่าการผ่าน (permeability) ที่สร้างขึ้นอยู่ในรูปของแอคติวิตี ผลการศึกษาพบว่าโพลิไวนิลแอลกอฮอล์เมมเบรนมีค่าการแยก (separation factor) ของกรดอะซิติก และเมทธิลอะซิเตตสูง แต่มีค่าน้อยสำหรับเมทธานอล และเมื่อทำการเปรียบเทียบระหว่างผลจากการจำลองกับผลจากการทดลองในการดำเนินงานแบบกึ่งกะพบว่าให้ผลที่สอดคล้องกัน เมื่อทำการเปรียบเทียบสมรรถนะระหว่างการดำเนินงานแบบต่อเนื่อง 2 แบบ คือ แบบถังกวนต่อเนื่องกับแบบท่อไหล ณ ค่าคงที่ของการดำเนินงานแบบไร้หน่วยค่าต่าง ๆ คือ ตัวเลขแดมโคเลอร์ (Damköhler number: Da) เรทเรโช (rate ratio: δ) อัตราส่วนสายป้อนและค่าการเลือกผ่านของเมมเบรน พบว่าผลของรูปแบบการไหลภายในเครื่องปฏิกรณ์ในการดำเนินงานแบบต่าง ๆ มีผลต่อสมรรถนะของเครื่องปฏิกรณ์เนื่องจากอิทธิพลของปฏิกิริยาและการผ่านของสารผ่านเมมเบรนและพบว่ามีบางช่วงของค่าการดำเนินงานที่การดำเนินงานแบบถังกวนต่อเนื่องเหมาะสมกว่าแบบท่อไหล การศึกษายังครอบคลุมถึงการเปรียบเทียบสมรรถนะของการดำเนินงานแบบต่อเนื่องของการสังเคราะห์เอสเทอร์ที่อยู่ในรูป $A + B \longleftrightarrow C + H_2O$ จากการศึกษาพบว่าเครื่องปฏิกรณ์แบบเพอร์แวบพอเรชันเมมเบรนมีสมรรถนะดีกว่าเครื่องปฏิกรณ์ทั่วไปในช่วงค่าคงที่สมดุลของปฏิกิริยาต่ำ ๆ และการดำเนินงานแบบท่อไหลเหมาะสมในช่วงที่สามารถควบคุมภาวะการดำเนินงานได้ อย่างไรก็ตามถ้าดำเนินงานช่วงเรทเรโชสูง ๆ พบว่าการดำเนินงานแบบถังกวนต่อเนื่องเหมาะสมกว่าการดำเนินงานแบบท่อไหล

ภาควิชา......วิศวกรรมเคมี..........   ลายมือชื่อนิสิต...

สาขาวิชา.....วิศวกรรมเคมี..........   ลายมือชื่ออาจารย์ที่ปรึกษา.............................

ปีการศึกษา..........2546............

JITKARUN PHONGPATTHANAPANICH: MATHEMATICAL MODELING OF PERVAPORATION MEMBRANE REACTOR FOR COMPARISON OF THE PERFORMANCES BETWEEN CONTINUOUSLY-STIRRED AND PLUG FLOW MODES FOR ESTERIFICATION REACTIONS.

THESIS ADVISOR: ASSOC. PROF. SUTHICHAI ASSABUMRUNGRAT, Ph.D., 91 pp. ISBN 974-17-3740-8

The performances of pervaporation membrane reactors with different modes of operation are discussed in this thesis. For the synthesis of methyl acetate (MeOAc) from methanol (MeOH) and acetic acid (HOAc) in pervaporation membrane reactors (PVMRs), three modes of PVMR operation: i.e. semi-batch (SB-PVMR), plug-flow (PF-PVMR) and continuous stirred tank (CS-PVMR) are considered. Mathematical models for different PVMR modes are developed using the kinetic parameters of the reaction over Amberlyst-15 and permeation parameters for a polyvinyl alcohol (PVA). Both of the reaction and permeation rates are expressed in terms of activities. The PVA membrane shows high separation factors for HOAc and MeOAc but very low for MeOH. The simulation results of SB-PVMR mode show quite good agreement with the experimental results. The study focuses on comparing PVMR performances between two modes of continuous flow operation for various dimensionless parameters, such as Damköhler number (Da), the rate ratio (δ), the feed composition and the membrane selectivity. Flow characteristic within the reactors arisen from different operation modes affects the reactor performance through its influences on the reaction and permeation rates along the reactor. There are only some ranges of operating conditions where CS-PVMR is superior to PF-PVMR. The study is extended to consider the case with a general form of esterification reaction, $A + B \longleftrightarrow C + H_2O$. The analysis shows that superiority of PVMR compared to conventional reactors is pronounced for the case with low values of K_{eq}. For all levels of K_{eq}, PF-PVMR is a favorable mode of operation as long as the operating conditions can be adjusted at a suitable condition. However, if the reactor is operated at relatively high value of δ, CS-PVMR is more suitable for the operation compared to PF-PVMR.

Department ….……Chemical Engineering… ...   Student's signature ……………………

Field of Study …Chemical Engineering…..   Advisor's signature ……………………

Academic year …………2003……………

ACKNOWLEDGEMENTS

TABLE OF CONTENTS

TABLE OFCONTENTS (Cont.)

TABLE OF CONTENTS (Cont.)

LIST OF TABLES

LIST OF FIGURES

LIST OF FIGURES (Cont.)

LIST OF FIGURES (Cont.)

NOMENCLATURE

a_i	activity of species i	[-]
a_i'	modified activity of species i $(=K_i a_i/M_i)$	[mol/kg]
A	effective surface membrane area	[m^2]
D	diffusivity coefficient	[m/s]
Da	Damköhler number $(=kW/F_{A,0})$	[-]
E_a	activation energy	[J/mol]
c_i	concentration of species i	[mol/m^3]
F_i	molar flow rate of species i in the reaction side	[mol/s]
$\overline{F_i}$	dimensionless mole flow rate of species i in	
	the permeate side	[-]
J_i	permeate flux of species i	[mol/m^2.s]
k	reaction rate constant	[mol/(kg.s)]
K_{eq}	equilibrium constant	[-]
K_i	adsorption parameter of species i	[-]
l	membrane thickness	[m]
M_i	molecular weight of species i	[kg/mol]
N_i	number of mole of species i in the reactor	[mol]
P_i	permeability coefficient of species i	[mol/(m^2.s)]
Q_i	molar flow rate of species i in the permeate side	[mol/s]
$\overline{Q_i}$	dimensionless molar flow rate of species i in	
	the permeate side	[-]
r	reaction rate	[mol/(kg.s)]
R_g	gas constant $(=8.314)$	[J/(mol/K)]
S	solubility coefficient	[mol/m]
t	reaction time	[s]
T	operating temperature	[K]
W	catalyst weight	[kg]
X_i	conversion base on reactant i	[-]

x_i	mole fraction of species i in liquid mixture	[-]
X_{eq}	equilibrium conversion	[-]

Greeks letters

α_i	separation factor of species i	[-]
δ	rate ratio ($P_{H_2O}A/kW$)	[-]
γ_i	activity coefficients of species i	[-]
ν_i	stoichiometric coefficient	[-]
υ	dimensionless axial coordinate	[-]
ξ	factor multiplying with the separation factor	[-]

Subscripts

0	initial value at $t = 0$
d	desired reagent to be removed
i	species i
H_2O	water
$HOAc$	acetic acid
$MeOAc$	methyl acetate
$MeOH$	methyl alcohol

CHAPTER I

INTRODUCTION

Integration of a chemical reactor and a separation unit into a single unit operation presents one of the most important trends in today's chemical engineering and process technology due to increased worldwide production competition. Many innovative processes and technologies offer intensive improvements in chemical manufacturing and processing which lead to a significant reduction in capital investment by decreasing equipment volume and number of required unit operations and reduction in operating cost which may be caused by a reduction of raw material use, diminution of recycle streams by higher rates of conversion, improvements in selectivity and energy integration and so on.

Multifunctional reactor is one type of the process intensification where the reaction function is combined with one or more functions that would be conventionally performed in separated equipment. In most case the reaction and separation are integrated to instance a shift of the reaction product composition beyond the equilibrium by internal separation or enhancement of the separation efficiency by a chemical reaction. This unit can be called as reactive separations or separative reactors.

Various multifunctional reactors have been proposed, for examples, chromatographic reactor, pressure swing reactor, thermal swing reactor, reactive distillation and membrane reactors. Substantially, they have many advantages over conventional processes. The capital investment is smaller because the separation unit is combined with the chemical reaction into a single process unit and the operating cost is lower due to higher performance.

A pervaporation membrane reactor (PVMRs) is one type of the multifunctional reactors that combine the chemical reaction and separation by pervaporation into a single unit. The pervaporation is a membrane separation process

which separates liquid mixtures that are difficult or not possible to separate by conventional methods. In the PVMRs, one or more products in a reaction liquid mixture contacting on one side of a membrane permeate preferentially through the membrane and the permeate stream is simultaneously removed as a vapor from the other side of the membrane while the reaction occurs.

As a result, the forward reaction can be enhanced. The advantages of this reactor are as follows (a) undesired side reactions can be suppressed; (b) the simultaneous removal of a product (usually water) from the reactor enhances the conversion; (c) the heat of reaction can be used for separation thus it is more energy-efficient and economically competitive than conventional separation means such as distillation; (d) the percents conversions of reactant are higher than percents conversion at thermodynamic equilibrium or complete reaction in some cases.

Condensation reactions such as acetalisation, ketalisation, esterification and etherification are normally limited by thermodynamic equilibrium and produce water as a byproduct. The reaction can be expressed in a general form as

$$A + B \leftrightarrow C + H_2O \tag{1-1}$$

High yield can be obtained by adding an excess of one reactant or by constantly removing water from the reaction mixture in order to shift the reaction to product side. By selecting a suitable membrane with good thermal stabilization, acid resistance, permselectivity and permeability, the PVMRs can significantly improve the reaction yield.

The PVMRs can be operated in various modes such as semi-batch (SB-PVMR) mode and continuous mode which includes continuously-stirred (CS-PVMR) and plug flow (PF-PVMR) modes. Although the continuous mode is more practical in an industrial-scale production, most researchers have studied the PVMRs in the semi-batch mode because it is easy to operate and requires fewer amounts of reactants. There are a few works considering the PVMRs in continuous mode; however, there has been no effort to compare the performances between the two

continuous modes of PF-PVMR and CS-PVMR. It is well recognized for a conventional reactor that the plug flow mode is superior to the continuously-stirred mode in term of obtainable conversion. However, for the PVMRs, it is more complicated because the presence of product removal via a membrane, which also depends on the mode of operation, needs to be taken into account.

It is the subject of this research to compare the performance of PVMRs under these two continuous modes. The comparison was carried out by computer simulation using the production of methyl acetate from methanol and acetic acid as an example reaction. Mathematical models of the PVMRs with different modes were developed using kinetic parameters of the reaction from literature and permeation parameters from our experimental studies. In addition, the comparison was extended to reactions in the general form, $A + B \longleftrightarrow C + H_2O$ so that wider ranges of operating parameters were considered.

CHAPTER II

THEORY

This chapter provides some background information on membrane definition, pervaporation process, membrane reactor and pervaporation membrane reactor. Details are as follows.

2.1 Membrane Definition

A membrane is a permeable or semi-permeable phase, often in the form of a thin film deposited on a support material as shown in Figure 2.1. It can be made from a variety of materials ranging from inorganic solids to different types of polymers. The main function of membrane is to control the exchange of mass between two adjacent fluid phases as shown schematically in Figure 2.2. For this function, the membrane must be able to act as a barrier, which separates different species either by sieving or by controlling their relative rate of transport through itself. The separation by membrane results in a fluid stream (defined as the retentate), which is depleted from some of its original components, and another fluid stream (defined as the permeate), which is concentrated in these components. Exchange between the two bulk phases across the membrane is caused from the presence of a driving force, which is typically associated with a gradient of pressure, concentration, temperature and electrical potential, etc. The types of membranes used for separation can be classified using different criteria such as by membrane structure (porous and non-porous) and by type of material used to prepare the membrane (organic, polymeric, inorganic, metal, etc.). The ability of a membrane to affect separation of mixtures is determined by two parameters, its permeability, defined as the flux, and selectivity, defined as the ratio of the individual permeabilities for the two species.
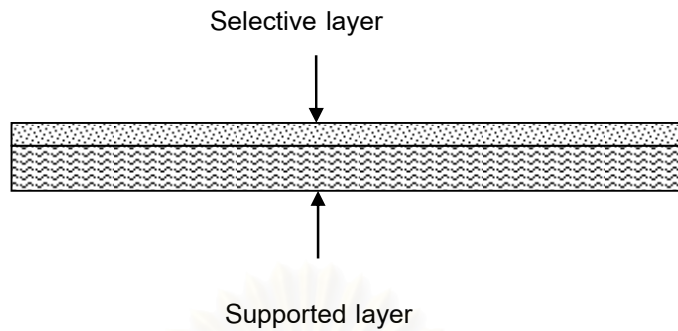
Figure 2.1 Cross-section of membrane
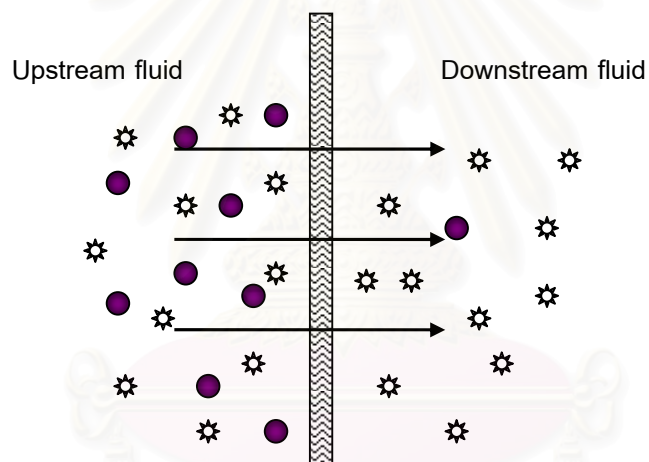
Figure 2.2 Basic membrane separation principle

2.2 Pervaporation process

2.2.1 Definition of pervaporation process

Pervaporation is a membrane separation process for separation of liquid mixtures. In the process, a liquid feed mixture is in contact with one side of a permselective dense membrane in a membrane module. Partial vapour pressure of

each component near the membrane surface is assumed at its saturation vapor pressure. A gradient in vapor pressure between the feed and the permeate sides of the membrane is a driving force for the permeation and it is maintained at high value by reducing the permeate side pressure. The permeate leaves the membrane as a vapour and is usually condensed and removed from the system as liquid. Heat necessary for evaporation of the permeate stream has to be transported through the membrane, and this transport of energy is coupled to the transport of matter. The evaporation enthalpy is taken from the sensible heat of the liquid feed mixture, leading to a reduction in the liquid mixture temperature. It makes pervaporation unique compared to all other transport processes involving in the membrane processes. A schematic of the pervaporation process is shown in Figure 2.3.
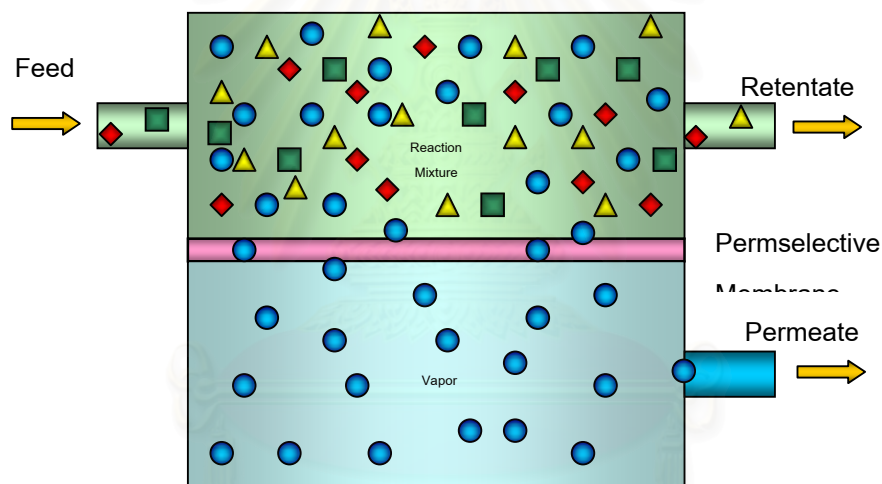
Figure 2.3 Schematic diagram of a pervaporation process

2.2.2 Transport in membrane

Transport of a component through a membrane in the pervaporation process can be described by the solution-diffusion model (Feng *et al.*, 1997). The mechanism consists of three consecutive steps (see Figure 2.4) as follows:

1) sorption of reagent from the liquid feed to the membrane

2) diffusion of reagent in the membrane and

3) evaporation or desorption of reagent in vapor phase from the downstream side of the membrane.

It is assumed that a component of the feed having a high affinity to the membrane is easily and preferentially adsorbed and dissolved in the membrane substance. Swelling effect is a major problem for pervaporation membrane compared to membranes for other membrane processes. This is because the membrane contacts with a high density fluid at high temperature.
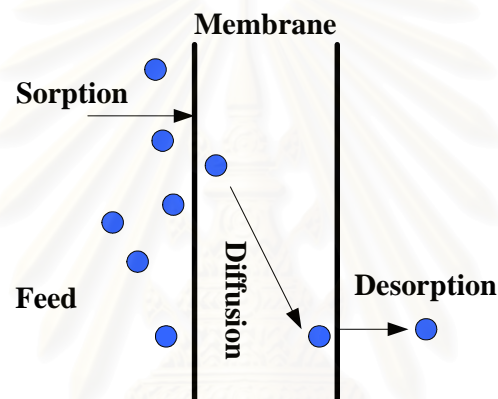
Figure 2.4 Schematic of pervaporation transport by solution-diffusion mechanism

Following a concentration gradient, the components migrates through the membrane by a diffusion process and are desorbed at the downstream side of the membrane into a vapour phase. In the pervaporation, the components passing through the membrane are sorbed out of a liquid phase but desorbed into a vapour phase.

Substances with lower or no solubility in the membrane material cannot be dissolved or slightly dissolved and thus the transport rate is low. As the diffusion coefficients of small molecules in a polymer matrix do not differ significantly, the separation characteristics of the membrane is primarily governed by the different

solubilities of the components in the membrane material and to a lesser extent by their diffusion rates.

The transport of a single component through a nonporous homogeneous membrane has been relatively well described. The concentration dependence of diffusivity is often expressed by exponential or linear forms. Assuming thermodynamic equilibrium exists at both membrane interfaces, the steady-state flux equation can be readily derived on the basis of Fick's equation for one-dimensional diffusion normal to the membrane surface. For binary mixtures, the mass transport is complicated by the permeant-permeant and permeant-membrane interactions, and no overall explaining theory exists.

It is noted that using the same approach as in single-component pervaporation, the solution-diffusion model has been modified by introducing different empirical parameters, most of which arise from the concentration dependence of diffusivities. Assuming that the diffusivities of individual permeants are proportional to the total concentration of permeants in the membrane. However, this model does not apply to non-ideal cases such as the pervaporation of alcohol/water mixtures. The concentration dependence of diffusivity is due at least in part to the plasticizing action of the permeants on the polymer, while different components may have different plasticizing effects. Hence, it is generally not appropriate to assume the contribution of permeants to their diffusivities to be linearly additive.

Further, as commonly observed, diffusivities are very sensitive to permeant concentration, especially when the membrane has a strong affinity to the permeating species. A simple linear relationship is often inadequate to describe the concentration dependence of diffusivity.

2.2.3 Characterization of membranes

2.2.3.1 Permeability and permeation rate

The phase change of the permeating species is one of the most distinguishing features of pervaporation. Based on the solution-diffusion model, the flux equation can be written as (Wijmans and Baker, 1995):

$$J_i = \frac{P_i}{l}(c_{io} - \frac{p_{il}}{H_i})$$ (2-1)

where c_{io} is the concentration of components i at the membrane surface and p_{il} is the partial vapor pressure of the permeant at the permeate side and l is the membrane thickness. P_i is the permeability coefficient of the membrane with respect to the driving force expressed in terms of partial vapor pressure and is related to the solubility coefficient (S) and diffusivity coefficient (D).

In the pervaporation process, when the permeate pressure (p_{il}) is kept at low value, the Equation 2-1 can be expressed as:

$$J_i = \frac{P_i}{l}c_{io}$$ (2-2)

and the permeation rate can be expressed as

$$Q_i = P_i A c_i$$ (2-3)

where Q_i and c_i are the permeate rate and the concentration of component i, respectively. A is effective membrane surfaces.

The permeability in Equations 2-1 to 2-3 are defined as:

$$P_i = D_i S_i$$ (2-4)

where D and S are normally dependent on temperature and the temperature dependence can be expressed as Equations 2-5 and 2-6, respectively.

$$D_i = D_{i,0} \exp(-\frac{E_{a_D}}{R_g T})$$ (2-5)

$$S_i = S_{i,0} \exp(-\frac{E_{a_S}}{R_g T})$$ (2-6)

Thus, the permeability can be written as the following equation.

$$P_i = P_{i,0} \exp(-\frac{E_a}{R_g T})$$ (2-7)

2.2.3.2 Membrane selectivity

Membrane selectivity of component i is defined as the ratio of the permeability of a desired component to be removed to that of the component i as follow:

$$\alpha_i = \frac{P_d}{P_i}$$ (2-8)

where α_i is the separation factor, P_d is the permeability of the desired component to be removed and P_i is the permeability of the component i.

2.2.3.4 Pervaporation process configurations

Transport through pervaporation membrane is produced by maintaining a vapor pressure gradient across the membrane. Figure 2.5 shows three potential ways to achieve the required vapor pressure gradient.

1) Vacuum driven pervaporation: This method is applicable when the volume of permeating vapour is relatively small. Although it is not a practical choice due to high energy consumption, this method is usually employed for small-scale operation in laboratory.

2) Temperature gradient driven pervaporation: The partial vacuum can be created by condensing the vapor into liquid. This method is preferable for commercial operations, because the cost for providing the required cooling is much less than the cost of a vacuum pump and the process is operationally reliable.

3) Carrier gas pervaporation: The permeate side of membrane is swept with an inert gas in which the partial vapour pressure of the critical component is kept sufficiently lower than that on the feed side. This method is attractive if the permeate has no value and can be discarded without condensation.
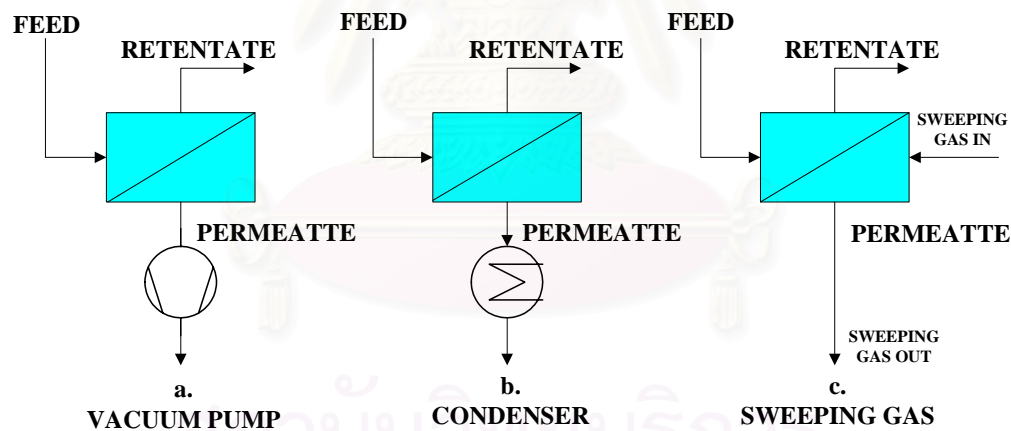
Figure 2.5 Modes of operation at the permeate side

2.2.4 Applications of Pervaporation

The applications of pervaporation process can be defined according to two different membrane classes as follows.

2.2.4.1 Organophilic membrane

Organophilic membranes are mostly applied for removal of volatile organic components (VOC's) from gas stream like waste air or nitrogen. Main applications are treatment of streams originating from evaporation of solvents in coating processes in film and tape production, from purge of products like polymers, from breathing of solvent storage tanks and especially from loading and unloading of gasoline tanks in tank farms.

2.2.4.2 Hydrophilic membrane

The application of hydrophilic membrane pervaporation can be separated in three purposes as:

1. Solvent dehydration: such as the dehydration of alcohols.
2. Removal of water from reaction mixtures.
3. Organic-organic separation: such as removal of methyl alcohol form trimethyl borate.

2.3 Membrane reactor

Membrane reactor couples a membrane separation process with a reactor into one unit operation. General advantages of membrane reactors as compared to sequential reaction-separation system are:

- o Increased reaction rate
- o Reduced by-product formation
- o Lower energy requirement
- o Possibility of heat integration

2.3.1 Basic functions of membrane in membrane reactor

The basic functions of the membrane in membrane reactors as various phases of operation can be divided in to (Figure 2.6):

- o Selective and non-selective addition of reactants
- o Selective and non-selective removal of reaction products
- o Retention of the catalyst

	L/L	L/G	G/G
Addition of reactant	✔	✔	✔
Removal of product	✔	✔	✔
Catalyst retention	✔	✔	✔

Remark: ✔ mean that the function of membranes able to apply to these phase

Figure 2.6 Basic functions of membranes in membrane reactor

As the membrane acts as a separating medium between two flow compartments, these basic functions can be applied to liquid/liquid, gas/liquid and gas/gas systems, respectively.

Based on a major division by membrane function in the reactor illustrating the importance of the use of membranes for combining reaction and separation. The following subjects will give an overview of the applications of membranes, for chemical reaction.

2.3.1.1 Membrane for controlled introduction of reactants

The major advantage of using membranes for the addition of reactants comprises the independent control of the concentration levels of each reactant in the reaction zone. One reactant can be fed along the length of a reactor, as shown in Figure 2.7. This is commonly done in a tube and shell configuration. An additional advantage is the possibility to apply a permselective membrane for purification of a reactant from mixed stream before addition into the reaction zone. Also, the membrane can be used for the coupling of two reactions by physically separating the two reaction media and introducing the product of one reaction as a reactant for the second reaction, as shown in Figure 2.8.
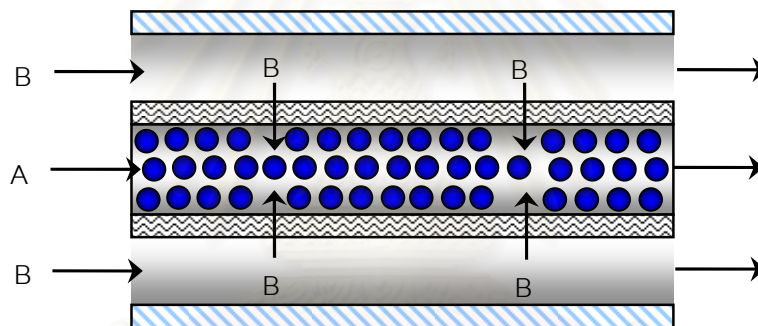
Figure 2.7 Membrane for the addition of reactants feed
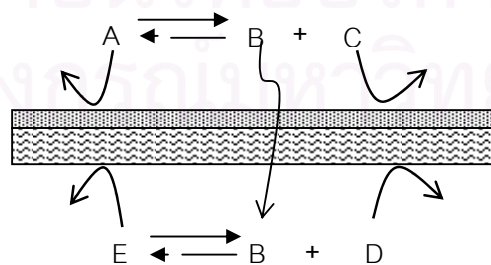
Figure 2.8 Membrane used for the coupling of two reactions

2.3.1.2 Membrane for separation of products

In general, a reversible reaction such as $A + B \longleftrightarrow C + D$ is often limited in conversion or yield by the reaction equilibrium. Removal one or both products by a membrane can increase the conversion as the reversible reaction is shifted to the right, as shown in Figure 2.9.

Additionally, undesirable side reactions such as the formation of component E in Equation 2-10 can be avoided by the separation of product C via a membrane. In consecutive catalytic reactions as illustrated in Equation 2-11, the desired intermediate product B can be obtained by selective removal of B from the reaction zone (as shown in Figures 2.10 and 2.11, respectively).

$$B + D \longleftrightarrow E \tag{2-10}$$

$$A \rightarrow B \rightarrow C \tag{2-11}$$
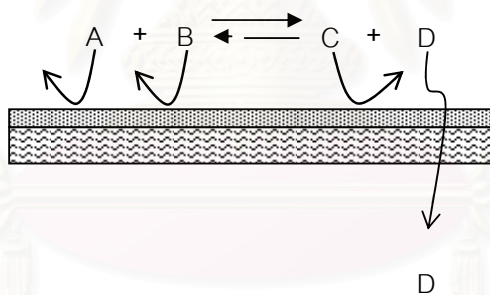
Figure 2.9 Membrane used for selective removal of products
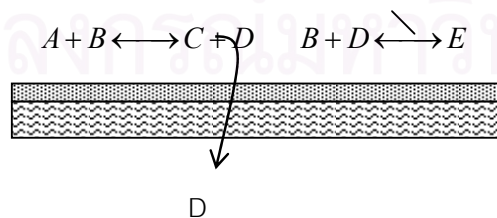
Figure 2.10 Membrane used for prevent undesirable side reactions

$$A \rightarrow B \rightarrow C$$

$$B$$
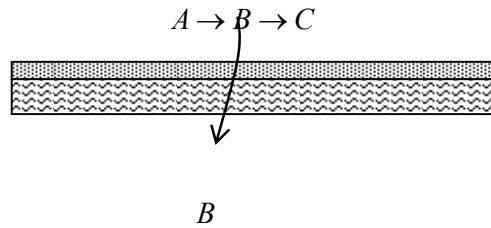
Figure 2.11 Membrane used for intermediate product removal

2.3.1.3 Membrane for catalyst retention

With respect to catalytic membrane reactors, processes can be divided into homogeneously and heterogeneously catalyzed reactions, as Figure 2.12. In homogeneously catalyzed processes, the membrane modules can be used in loop reactors. For heterogeneously catalyzed reactions several configurations are possible.

For this purpose, three basic types of catalytic systems can be distinguished:

1) A membrane can be used to retain a mobile catalyst, thus keeping the catalyst in the reaction fluid.
2) A catalyst can be immobilized in a porous membrane structure
3) The membrane itself can act as the catalyst
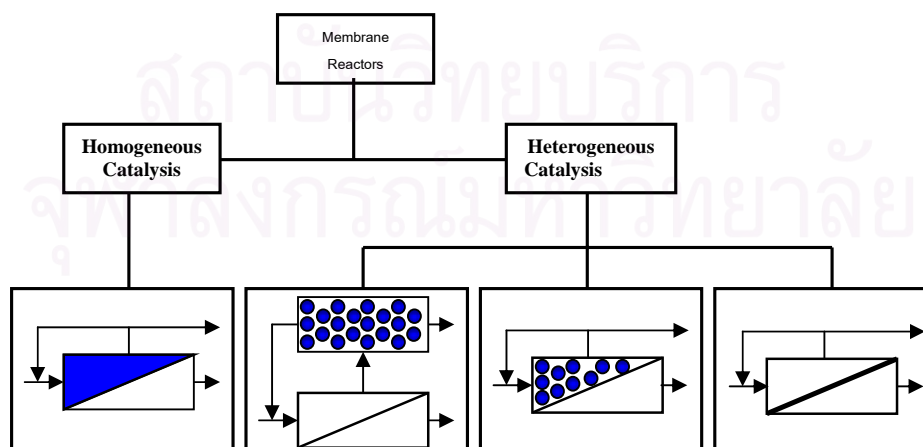
Figure 2.12 Classification of catalytic membrane reactors

2.4 Pervaporation membrane reactors

Pervaporation membrane reactor, one type of the membrane reactors, combines chemical reaction unit and pervaporation unit into a single unit. The concept of this reactor was first proposed by Jenning and Binning in 1960. While a reaction takes place in a liquid phase, a by-product (usually water) is removed through a membrane to the permeate side. As a result, the reaction can go forward to the product side.

Recently, most of pervaporation membrane reactors are used in condensation reactions which are equilibrium-limited reactions and water is produced as a by-product. Typical condensation reactions include:

Esterification: $R' - COOH + HO - R \leftrightarrow R'COOR + H_2O$ (2-12)

Acetalisation: $R' - CHO + 2HO - R \leftrightarrow R'CH - (OR)_2 + H_2O$ (2-13

Etherification: $R' - OH + R - OH \leftrightarrow R' - O - R + H_2O$ (2-14)

Ketalisation: $R'R''CO + 2HO - R \leftrightarrow R'R''C(OR)_2 + H_2O$ (2-15)
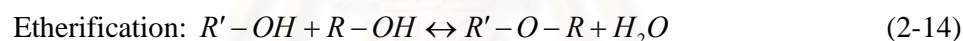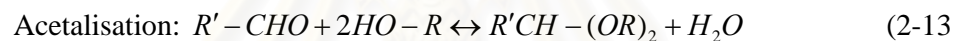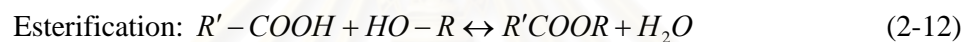
Removal of water from the mixture will shift the reaction equilibrium to the side of the desired product. If one of the reactants is used at surplus over the stoichiometry, nearly full conversion of the other, usually the more valuable reactant can be achieved, resulting on leading to a much higher yield of the desired product. Furthermore, the desired product has no longer to be separated and purified from a four component mixture (the two reactants, the desired product and water). Since water is removed through the pervaporation membrane and one of the reactants nearly totally converted, only the separation of the product from the surplus reactant is required. The benefit from reduction in downstream purification load may be even at least as economically as the higher product yield.

The pervaporation membrane reactor is used for two purposes as follows:

1) Yield-enhancement of equilibrium limited reactions
2) Selectivity enhancement

The advantages of the pervaporation membrane over the conventional reactor can be summarized as follows

1) Unlike a conventional separation processes, the separation of azeotropic mixture is possible.
2) Consuming energy lower than other separation processes.
3) Flexible to increase or decrease the productivity by add or remove pervaporation unit.

The integration of pervaporation with chemical reactor has been defined as two types (Lipnizki *et al*. 1999) as:

1) External integration: The pervaporation unit is installed out side the reactor to remove the product or by-product from within the reactor (or from a recycle loop around the reactor).
2) Internal integration: The pervaporation unit is combined with the reactor into single unit to remove the product or by-product directly from reaction mixture.

The basic layouts of both pervaporation membrane reactor configurations are illustrated in Figure 2.13.
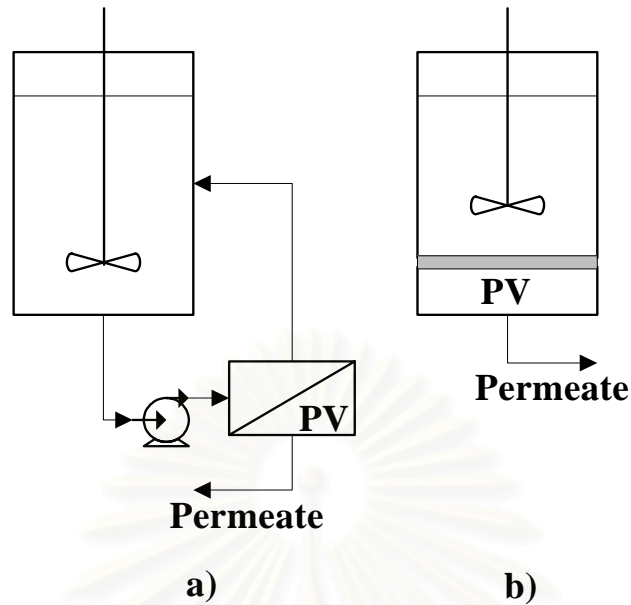
Figure 2.13 Configurations of a pervaporation membrane reactor with an external
pervaporation unit (a) with an internal pervaporation unit (b)

2.4.1 Performance of pervaporation membrane reactor

The performance of the pervaporation membrane reactor depends not only on
upon the physicochemical properties of the membrane, especially polymeric material,
and the structure of membrane but also upon the operating conditions, e.g.
temperature, downstream pressure and composition of mixture. The followings
summarize the effects of various factors on the performance of the pervaporation
process.

2.4.1.1 Physico-chemical properties

The permeation of solvents through a non-porous membrane usually can be
described in terms of sorption and molecular diffusion. The extent of sorption, also
called swelling, as well as the sorption selectivity is therefore determined by chemical
nature of polymer and that of the solvents.

2.4.1.2 Feed composition

A change in feed composition directly affects the sorption phenomena at the liquid-membrane interface. The sorption selectivity depends obviously on the influence of the interaction between components. The extent of swelling as well as the sorption selectivity depends on the structure of polymer network. The lower affinity to the membrane can penetrate into the swollen system, and contribute to better swelling.

2.4.1.3 Feed concentration

According to Fick's law, the permeation is proportional to the activity gradient across the membrane. Since the feed concentration directly affects the membrane activity, the increased feed concentration increases the driving force and the permeation flux through the membrane.

2.4.1.4 Operating temperature

The variation of permeation rate with follows from the operating temperature can be correlated with the Arrhenius' equation as expressed as Equation 2-8, higher permeation flux at higher temperature.

2.4.1.5 Downstream pressure

Pervaporation process controls downstream pressure by pumping the permeate from downstream interface in the vapor form to provide the driving force. The decreased vapor pressure in downstream compartment is equivalent to an increased driving force for components transportation.

CHAPTER III

LITERATURE REVIEWS

Pervaporation membrane reactor (PVMR) incorporates the pervaporation process, which shows advantages over conventional separation process such as lower energy consumption and capitals investment, ability on azeotrope mixture separation, etc., into reactors. There are a number of researchers focusing on PVMRs. In this chapter, literature reviews on application of PVMRs for esterification reactions and modeling of PVMRs are provided.

3.1 Pervaporation membrane reactor for esterification

Early researches on membrane reactors were popular in the field of biotechnology. Main functions of membranes are for immobililizing enzymes, recycling enzymes and other biocatalyst, and manipulating substrates and nutrients. Recently, a number of researches have moved membrane reactor applications to chemical reactions especially high temperature gas phase reactions such as catalytic dehydrogenation, hydrogenation and decomposition reactions. Limited numbers of researches have considered liquid phase reactions because of the lack of suitable membranes which have high permselectivity, good thermal and chemical resistances. Ultrafiltration can not be employed to separate liquid mixture due to its high porosity of the membrane. Although it is possible to use reverse osmosis to separate the mixture, unfavorably high operating pressure is required. Pervaporation, a promising process for separation of water/organics or organic/organic mixtures, was intensively studied in the past decades (Huang, 1991). Thus, there was an idea to combine pervaporation and chemical reaction in one unit called "pervaporation membrane reactor" (Jenninig and Sinning, 1960).

Recently, most pervaporation membrane reactors have been used for equilibrium-limited condensation reactions which produce water as a by-product. Table 3.1 shows examples of reactions and membranes. To achieve a high conversion and yield, it is customary to drive the reaction go forward to the ester or ether by either using a large surplus of one of the reactants or using other processes such as reactive distillation to accomplish in situ removal of product. However, the large surplus of reactant increases the cost for subsequent separation processes, while reactive distillation is effective when the difference between the volatility of product and the volatility of reactant are sufficiently large. In the case of azeotrope reaction mixtures a simple reactive distillation configuration is inadequate. In addition, when the reactive distillation is operated at large reflux ratio, high energy are consumed. PVMR is attractive because the pervaporation does not depend on the relative volatility of the components and the energy consumption is only a fraction of that required for the distillation since it involve only partial evaporative of the feed.

Esterification is intensively studied in pervaporation membrane reactors in the past decades. Because the reaction suffers from thermodynamic limitation and produces water as a by-product which can be selectively removed from the system by a pervaporation membrane. Various reactions have been considered.

TABLE 3.1 Examples of research in pervaporation aided esterification reaction

Reaction	Membrane	Reference
ethyl alcohol + acetic acid	Polyetherimide	Kita *et al.* (1988)
	Polyvinyl alcohol	Zhu *et al.* (1996)
	Zeolite T	Tanaka *et al.* (2001)
	H-ZSM-5	Bernal *et al.* (2002)
ethyl alcohol + oleic acid	Polyimide	
	Chitosan	Kita *et al.* (1987)
	Polyetherimide	Kita *et al.* (1988)
	Nafion	Okamoto *et al.* (1993)
	Perfluorated ion-exchange	
1-propanol + proionic acid	Polyvinyl alcohol	David *et al.* (1991)
2-propanol + proionic acid	Polyvinyl alcohol	David *et al.* (1991)
n-butanol + acetic acid	Polyvinyl alcohol	Lui *et al.* (2001)
benzyl Alcohol + acetic acid	Polyvinyl alcohol	Domingues *et al.* (1999)

The synthesis of ethyl oleate from oleic acid and ethyl alcohol by using *p*-toluenesulphonic acid as a catalyst and polyimide, chitosan, nafion, polyetherimide and perfluorateed ion-exchange as membranes were investigated (Kita *et al*., 1987, 1988; Okamoto *et al*., 1993). It was found that the polyetherimide membrane showed the highest permselectivity (Kita *et al*., 1988). Complete reaction was reached within 6 hours with excess ethyl alcohol.

The esterification of ethyl alcohol with acetic acid was investigated in a semi-batch mode using *p*-toluenesulfonic acid and polyetherimide membrane (Kita *et al.*, 1988). Subsequently, the same reaction operated under continuous plug flow mode was considered by Zhu *et al*. (1996). Using supported polyetherimide as a

membrane and sulfuric acid as a catalyst, the obtained conversions significantly exceeded the equilibrium value observed in a conventional plug flow reactor.

There was an attempt to study this reaction using a heterogeneous catalyst in the continuous tubular membrane reactor (Waldburger *et al.,* 1994). In the tube of membrane, hydrophilic polyvinyl alcohol (PVA) membrane was placed on a sintered tube as a support. When equimolar reactants were fed to the reactor, the yield of ethyl acetate was 92.1% with water concentration of 0.5 % by weight in the product stream. With a cascade of three membrane reactors, the ethyl acetate yield increased to 98.7% and the water concentration was reduced to 0.1% by weight. An economic assessment revealed that the pervaporation membrane reactor could cut energy cost by over 75% and operating costs by 50% when compared to the conventional processes.

Tanaka *et al.* (2001) applied the zeolite (T) membrane which has high chemical and thermal stability than a polymer membrane for the same reaction. Almost complete conversion was reached within 8 hours when initial molar ratios of alcohol to acetic were 1.5 and 2. The influence of operating parameters on variation in conversion with reaction time was investigated by means of simulation using the model assuming that the reaction rate obeyed second-order kinetics and the permeation flux of each component was proportional to its concentration.

David *et al.* (1991) studied the esterification of 1-propanol and 2-propanol with propionic acid to produce propyl propionate and *iso*-propyl propionate. Pervaporation membrane reactor with polyvinyl alcohol membrane was externally added to the reactor. The study revealed that the hybrid process was governed by four main parameters that influenced the conversion rate of pervaporation membrane reactor: in order of significance, these were temperature, initial molar ratio, surface membrane area to reaction volume ratio, and catalyst concentration.

Feng and Huang (1996) studied esterification facilitated by pervaporation. A batch pervaporation membrane reactor was selected as the model system to provide a fundamental understanding of the reactor behavior. The simulation showed that the conversion exceeding equilibrium limits can be achieved by using pervaporation to

remove water from the reaction mixtures and complete conversion of one reactant was obtained when the other was in excess. The membrane tolerated the presence of water, which can be either in the reaction medium or as impurity of the reacting reagent. It was found that there were upper and lower limits in performance of reactor facilitation with pervaporation. Membrane permeability, membrane area and volume of reaction mixtures to be treated were important operating parameters influencing the reactor behavior. Moreover, operating temperature influenced the reactor performance through its influences on reaction rate and membrane permeability.

The esterification of benzyl alcohol with acetic acid was studied in a pervaporation membrane reactor (Domingues *et al.*, 1999). A commercial GFT Pervap 1005 membrane was used to analyze its possible application on an industrial level. The results showed 96 % selectivity in water and 99 % conversion. A theoretical model was developed and the simulation results satisfactorily agreed with the obtained experimental results, thus allowing the prediction of the conversion variation with time.

There were attempts to study the parameters which influenced the performance of the pervaporation membrane reactor (Lui *et al.,* 2001). The separation characteristics of the cross-linked polyvinyl alcohol membrane were studied by separating of the liquid mixtures of both binary mixtures (water/acetic acid) and quaternary mixtures (water/acetic acid/*n*-butanol/butyl acetate). It was found that the permeation fluxes of water and acetic acid were present as function of compositions. A kinetic model equation was developed for the esterification of acetic acid with *n*-butanol catalyzed by $Zr(SO_4)_2.4H_2O$ and then it was taken as a model reaction to study the coupling of pervaporation with esterification. Experiments were conducted to investigate the effects of several operating parameters, such as reaction temperature, initial molar ratio of acetic acid to *n*-butanol, ratio of the membrane area to the reacting mixture volume and catalyst concentration on the pervaporation membrane reactor. The experimental results indicated that increasing the temperature accelerated the rate of water extraction faster than that of water production rate. But on the initial molar ratio, water production rate is decreased with the increase of initial molar ratio and, consequently, the rate of water removal was decreased. Water production rate was the same at various *S/V* but the rate of water removal was reduced

with the decrease of *S/V*. Water production rate was proportional to and increased with the increase of catalyst concentration, and thus resulting in the increase in water permeation flux.

Recently, there were studies that used a catalytically active membrane for synthesis of esters (Bernal *et al.*, 2002). Zeolite membrane, which was used for removing by-product water in several studies, was used as a catalyst in esterification and as a membrane by coating it on a tubular support. Water generated on the membrane can favorably transport to the permeate side. The conversion increased because a faster removal of water from the catalyst surface led to a higher turnover rate. However, the increased conversion was not higher than the equilibrium conversion due to the relatively low zeolite loading on the membrane. Moreover, the comparison of three reactor configurations i.e. (i) Fixed Bed Reactor (FBR) with the H-ZSM-5 catalyst packed as powder inside an impervious tube (ii) Zeolite Membrane Reactor (ZMR) with the H-ZSM-5 catalyst packed as powder inside a tubular Na-ZSM-5 membrane and (iii) Active Zeolite Membrane Reactor (AZMR) where there was no catalyst other than the H-ZSM-5 itself, were carried out. With the same amount of catalyst for all the cases, the results indicate that AZMR gives a significantly higher conversion compared to the conventional reactor and ZMR.

3.2 Modeling of pervaporation membrane reactor

There are a number of researchers studying PVMRs by computer simulation. Due to simplicity of a concentration-based model, many researchers have expressed the mathematical models in terms of concentration. By parametric studies, Feng and Huang (1996) reported that reaction and conversion rate can be enhanced that a complete conversion can be achieved if one reactant are in excess. The important parameters influenced the behavior of reactor are membrane permeability, membrane area to volume of reacting mixtures ratio and initial molar ratio. Furthermore, it was found that the operating temperature influenced both the reaction rate and membrane permeation rate. Domingues *et al.*, (1999) studied a pervaporation membrane reactor for the esterification of acetic acid with benzyl alcohol by applying *p*-toluenesulfonic acid as a catalyst. Xuehui and Lefu (2001) proposed the mathematic model of

pervaporation aided esterification of *n*-butyl alcohol with acetic acid by using polyvinyl alcohol as a membrane. Lui and Chen (2002) developed the mathematic models of esterification of acetic acid with *n*-butanol in the presence of $Zr(SO_4)_2.4H_2O$ coupled pervaporation. In all case, concentration-based models were used to determine the kinetic parameters. A theoretical model were developed and satisfactorily agreed with the obtained experimental results. Thus, several simulations were performed with obtained model to indicate the influence of the important parameters (Feng and Huang, 1996; Domingues *et al.*, 1999; Lui and Chen 2002). The membrane area to volume (*A/V*) or the membrane area to mass of reacting mixture (*A/M*). The efficiency of the process was strongly related to *A/V* or *A/M* ratio. Increasing the value of *A/V* or *A/M* ratio can efficiently shift the reaction equilibrium and obtain a reasonably pure ester directly after the reaction. Selection of the *A* and *V* values was determined from an economic point of view.

The synthesis of diethyltartarate from tartaric acid and ethyl alcohol was studied by Keurentjes *et al.* (1994). The equilibrium composition could be significantly shifted towards the final product diethyltartarate by integrating pervaporation, using a PVA composite membrane, into the process. The kinetic parameters were established. Both concentration-based and activity-based reaction rate constants and equilibrium constants were determined. The UNIFAC method was used to calculate activity coefficients in the activity-based model. It can be concluded that reaction rate constants determined in dilute solutions are capable of describing the reaction in a concentrated environment. This applies both for the activity-based description as well as for the concentration-based description. Although the activity coefficients involved differ significantly from unity, the effects of the individual activity coefficients are mutually compensated. Therefore, it is also possible to predict the reaction correctly when the concentration-based parameters are used.

A continuous pervaporation membrane reactor for the esterification of acetic acid with ethyl alcohol to produce ethyl acetate was studied by Zhu *et al.* (1996). A hydrophilic polymeric/ceramic composite membrane was used as a pervaporation membrane. For a range of experimental conditions reaction conversions were higher than the corresponding calculated equilibrium values. A model of pervaporation

membrane reactor in terms of activity was presented. It gave a good agreement with a set of experimental data.

Krupicka and Koszorz (1999) studied the same reaction and three-parameter model describing the concentration profiles in the process was developed. A comparison of the measured concentrations with those calculated according to the model shows sound agreement when the activities are used. The model is independent of the initial molar ratios due to the stability of thermodynamic and kinetic constants. Lim *et al*. (2002) reveals that despite of different dimensionless terms. The models take into account the non-ideal effect by expressing the reaction and permeation rates in terms of the activities. The reactor is assumed to behave as an ideal reactor and the concentration polarization effect is considered negligible. In addition, the membrane is assumed to be completely unreactive.

Kiatkittipong *et al.* (2002a, 2002b) developed the mathematic model of pervaporation membrane reactor coupled with etherification of ethyl alcohol with *tert*-butyl alcohol catalyzed by β-zeolite and polyvinyl alcohol as a membrane. The simulation results from developed activity-based model agreed with experimental result.

CHAPTER IV

EXPERIMENTAL

The experimental setups and procedures are described in this chapter. Details are given on materials and analysis method, batch reactor study, permeation study and pervaporation membrane reactor in the experimental of synthesis of methyl acetate from methyl alcohol and acetic acid on Amberlyst-15 ion exchange catalyst.

4.1 Materials

4.1.1 Chemicals

The details of chemicals used in experiments for the synthesis of methyl acetate from methanol and acetic acid in pervaporation membrane reactor are shown in Table 4.1

TABLE 4.1 Chemicals used in the synthesis of methyl acetate.

Chemical	Grade	Supplier
Methyl Alcohol	Analytic grade	Fluka
Acetic Acid	Analytic grade	Calro Erba
Methyl Acetate	Analytic grade	Fluka
Amberlyst-15	-	Fluka

4.1.2 Membrane

Polyvinyl alcohol (PVA) membranes (PERVAP 2201) purchased from Sulzer Chemtech GmbH-Membrane Systems were used as a hydrophilic membrane. The properties are described as follows.

TABLE 4.2 Polyvinyl alcohol (PVA) membrane (PERVAP 2201) properties

Code	PERVAP 2201
Main Application	Neutral solvents Reaction mixtures
Max. Temperature Long Term, K	373
Max. Temperature Short Term, K	378
Max. Water Content in Feed, % by w.	≤ 90
Major Limitation	
Aprotic Solvents (e.g. dimethylformamide ;DMF, dimethylsulfoxide;DMSO)	≤ 1 %
Organic Acid (e.g. acetic acid)	≤ 50 %
Formic Acid	≤ 0.5 %
Mineral Acid (e.g. H_2SO_4)	≤ 1 %
Alkali (e.g. NaOH)	≤ 10 ppm
Aliphatic Amines (e.g. Triethylamine)	≤ 50 %
Aromatic Amines (e.g. Pyridine)	≤ 50 %

4.2 Analysis method

Compositions of liquid mixture from experiments were analyzed by gas chromatography, Shimadzu model GC 8A, with Gaskuropack-54 packed column. Table 4.3 shows the operating conditions of the gas chromatography (see Appendix B for details on calibration of the gas chromatography).

TABLE 4.3 Operating condition of gas chromatography

Model	Shimadzu model GC 8A
Detector	TCD
Packed column	Gaskuropack 54
Column length	3 m
Mesh size of packing	60/80
Helium flow rate	30 ml/min
Column temperature	473 K
Injector temperature	493 K
Detector temperature	473 K

4.3 Permeation studies

Experiments on permeation of species in quaternary mixtures through the membrane were carried out to obtain the parameters of the permeation flux equation (pre-exponent (P_o) and activation energy (E_a)) and separation factor (α_i) of the membrane.

4.3.1 Experimental setup for permeation studies

The schematic diagram of the permeation experimental setup of the methyl acetate synthesis system is shown in Figure 4.1. A flat sheet polyvinyl alcohol (PVA) membrane, PERVAP 2201 purchased from Sulzur Chemtect GmbH Membrane Systems, with an effective area of 63 cm^2 was placed between two chambers and sealed with two silicone O-rings. A disk turbine was used to stir the liquid mixture in the upper chamber, retentate side, to ensure well-mixed condition while a condenser was affixed to the chamber to condense all vapors leaving the chamber. The lower chamber, permeate side, was fed with N_2 sweep gas at a constant molar flow rate of 8.9×10^{-5} mol/s to increase the driving force of the system. Both chambers were heated by circulated hot water feed to the chamber's jacket to keep the system at a constant temperature.

The bubble flow meter and a gas chromatography were used to measure the exit volumetric flow rate and its composition, respectively, to obtain the molar flux of each species.
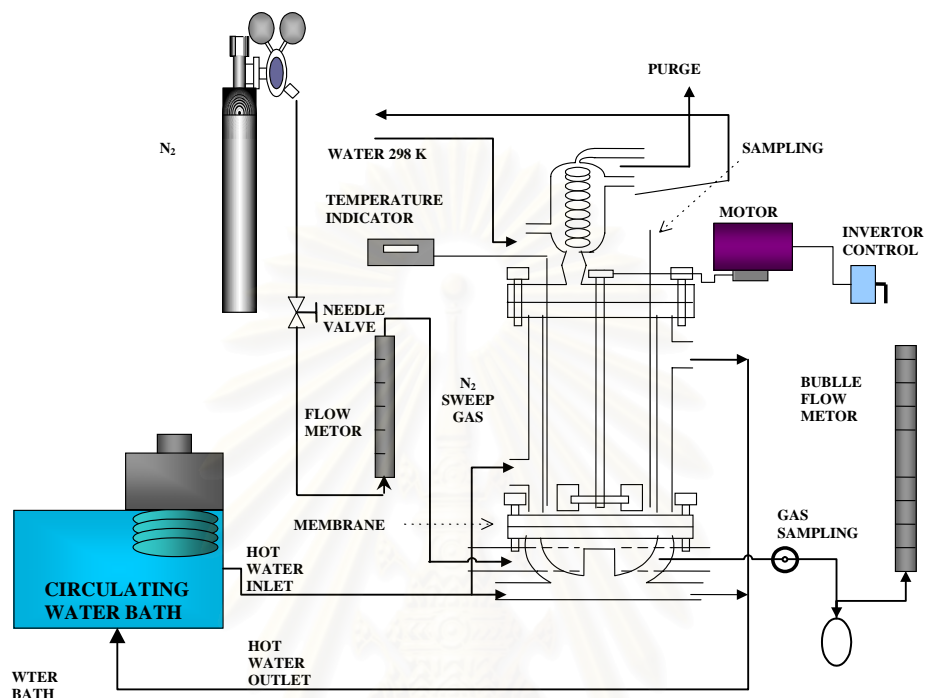
Figure 4.1 Schematic diagram of the permeation experimental setup of methyl acetate synthesis

4.3.2 Experimental procedure

1. The membrane was dried in an oven at 353 K for 3 hours before use to remove moistures in membrane.
2. N_2 sweep gas molar flow rate was adjusted to 8.9×10^{-5} mol/s and held for 2 hours to ensure that the flow was constant and to remove moisture in the permeate side.
3. A mixture of water/methanol/acetic acid/methyl acetate with known composition was added to the upper chamber and heated to constant temperature at $T = 323$, 333 and 343 K for experiments No.1, No.2 and No.3, respectively. After the temperature reached a desirable value, the system was held at that condition for 1 hour.

4. Permeate fluxes of each species were obtained by measuring the permeation flow rate by a bubble flow meter and its composition by the gas chromatography (sample gas = 2 ml) at different time until the contents of species checked by the gas chromatography were found to be constant.
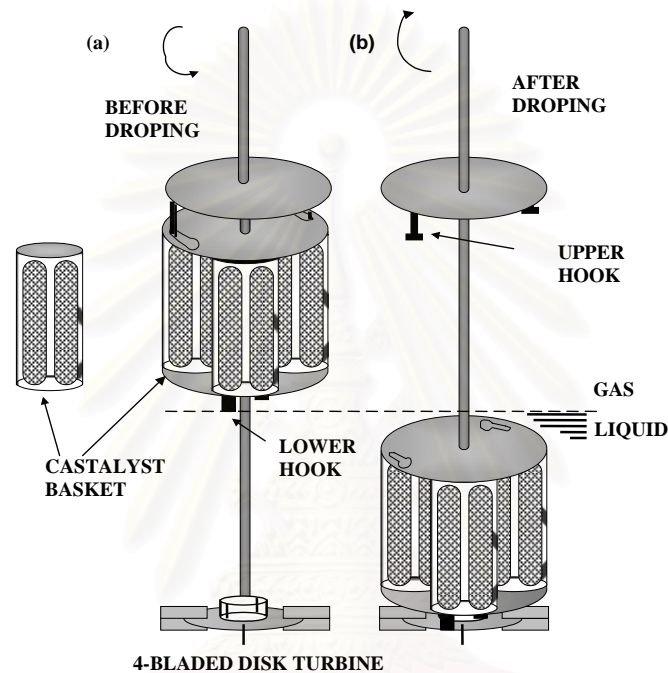
Figure 4.2 Detail of catalyst basket assembly.
(a) Before dropping
(b) After dropping

4.4 Pervaporation membrane reactor studies

Pervaporation membrane reactors were studied for correcting the developed models by compare the results between the experimental result with simulation result. The experiment and simulation temperatures used were at 333 K

4.4.1 Experimental setup for pervaporation membrane reactor studies

The pervaporation membrane reactor was carried out in the same apparatus used for the permeation study; however, the catalyst baskets (as illustrated in Figure 4.2) were equipped.

4.4.2 Experimental procedure for pervaporation membrane reactor studies

1. The membrane was dried in an oven at 353 K for 3 hours before use to remove the moistures in membrane.
2. N_2 sweep gas molar flow rate was adjusted to 8.9×10^{-5} mol/s and held for 2 hours to ensure that the flow was constant and to remove moisture in the permeate side.
3. 15 grams of catalyst (Amberlyst-15) was packed in four baskets held above the liquid level of reactant mixture by upper hooks as shown in Figure 4.2 (a) to prevent the reaction occurring.
4. 1 mole of methyl alcohol and 1 mole of acetic acid were pre-heated at a desired temperature, $T = 333$ K.
5. Four-bladed disk turbine was used to stir the liquid mixture. The reaction was started by inverting the direction of agitation so that the frame of baskets dropped into the liquid mixture. The lower hooks were securely connected with slots on the disk turbine and the frame was rotated without slip as shown in Figure 4.2 (b).
6. A liquid sample of 1 cm^3 was taken to measure compositions of acetic acid, methyl alcohol, methyl acetate and water at different reaction times: i.e. 0, 10, 20, 30, 40, 50, 60, 90, 120, 180, 240, 300 minutes.

CHAPTER V

MATHEMATICAL MODELS

The mathematical models were developed to investigate the performance of pervaporation membrane reactor in continuous operation, CS-PVMR and PF-PVMR. The first case are investigate the specific reaction, the esterification of methyl acetate in pervaporation membrane reactor then investigate the general reaction.

5.1 Esterification of methyl acetate in pervaporation membrane reactor

The esterification of methyl acetate from methyl alcohol and acetic acid over Amberlyst-15 ion-exchange resin catalyst was chose to investigate the performance

5.1.1 Kinetic of reaction

The reaction taking place in the reactor can be summarized as follows;
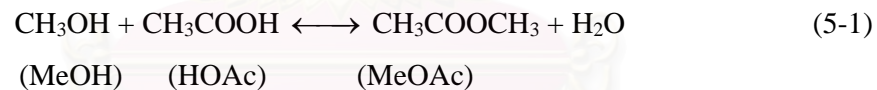
$$CH_3OH + CH_3COOH \longleftrightarrow CH_3COOCH_3 + H_2O \qquad (5\text{-}1)$$
$$(MeOH) \quad (HOAc) \qquad (MeOAc)$$

The rate model and the kinetic parameters of the reaction over Amberlyst-15 are expressed as follows (Popken *et al.,* 2000).

$$r = \frac{k(a'_{HOAc}\, a'_{MeOH} - \dfrac{a'_{MeOAc}\, a'_{H_2O}}{K_{eq}})}{(a'_{HOAc} + a'_{MeOH} + a'_{MeOAc} + a'_{H_2O})^2} \qquad \textbf{(5-2)}$$

with
$$a'_i = \frac{K_i a}{M_i}$$

$$k = 8.497 \times 10^9 \exp(-\frac{60470}{R_g T}) \tag{5-3}$$

$$K_{eq} = 7.211 \times 10^{-2} \exp(\frac{3260}{R_g T}) \tag{5-4}$$

and $K_{HOAc} = 3.15$, $K_{MeOH} = 5.64$, $K_{MeOAc} = 4.15$, $K_{H2O} = 5.24$.

The activity (a_i) can be calculated using the UNIFAC method as shown in Appendix B.

5.1.2 Rates of pervaporation

Assuming that partial pressure of all species in the permeate side was low, the permeation rate of species i through the membrane can be expressed as

$$Q_i = A P_i a_i \tag{5-5}$$

The relationship between the permeability coefficient and operating temperature can be correlated by the Arrhenius equation

$$P_i = P_{i,o} \exp(-\frac{E_a}{R_g T}) \tag{5-6}$$

5.1.3 Modeling of pervaporation membrane reactors

Three operation modes of PVMRs; i.e. semi-batch (SB-PVMR), continuous stirred tank (CS-PVMR) and plug flow (PF-PVMR) were considered in the study. The mathematical models were obtained from material balances around the reactors, assuming the reactors behaved ideally. In addition, isothermality, negligible pressure drop, negligible heat- and mass-transfer resistances aside from the permeation process and no coupling effect of mixtures on the permeability were assumed. The sets of equations for different operating modes can be summarized as follows.

$$SB\text{-}PVMR: \quad \frac{\mathrm{d}}{\mathrm{d}t}N_i = v_i Wk \frac{(a'_{HOAc}\,a'_{MeOH} - \dfrac{a'_{MeOAc}\,a'_{H_2O}}{K_{eq}})}{(a'_{HOAc} + a'_{MeOH} + a'_{MeOAc} + a'_{H_2O})^2} - AP_i a_i \tag{5-7}$$

$$PF\text{-}PVMR: \quad \frac{\mathrm{d}}{\mathrm{d}\upsilon}\overline{F}_i = v_i Da \frac{(a'_{HOAc}\,a'_{MeOH} - \dfrac{a'_{MeOAc}\,a'_{H_2O}}{K_{eq}})}{(a'_{HOAc} + a'_{MeOH} + a'_{MeOAc} + a'_{H_2O})^2} - \frac{Da\delta a_i}{\alpha_i} \tag{5-8}$$

$$\frac{\mathrm{d}}{\mathrm{d}\upsilon}\overline{Q}_i = \frac{Da\delta a_i}{\alpha_i} \tag{5-9}$$

$$CS\text{-}PVMR: \quad \overline{F}_{i,o} - \overline{F}_i + v_i Da \frac{(a'_{HOAc}\,a'_{MeOH} - \dfrac{a'_{MeOAc}\,a'_{H_2O}}{K_{eq}})}{(a'_{HOAc} + a'_{MeOH} + a'_{MeOAc} + a'_{H_2O})^2} - \frac{Da\delta a_i}{\alpha_i} = 0 \tag{5-10}$$

Various design operating parameters and physical property parameters are characterized in dimensionless groups to facilitate parametric analysis for the comparison of reactor performances under different operation modes.

1) Damköhler number, Da $(=kW/F_{HOAc,0})$ is a measure of the residence time,
2) the rate ratio, $\,(=P_{H_2O}A/kW)$ is a measure of the ratio between permeation rate and reaction rate,
3) the separation factor, $\,_i(=P_{H_2O}/P_i)$ is a measure of membrane selectivity.

Some of the above assumptions may not be valid in all ranges of operating conditions of the PVMRs. Coupling effects in liquid mixtures are known to have a significant impact on actual permeabilities. For PF-PVMR, the axial pressure drop can be significant at high Reynolds numbers and the mass transfer resistance between the liquid bulk and the surface of catalyst particles and also of the membrane surface becomes significant at large value of Da. In addition, non-ideal conditions such as complete mixing in CS-PVMR; non-isothermal condition; radial and axial gradient of concentration and temperature, should exist in actual operation of both modes. More rigorous models should be investigated in future studies.

EQUATRAN-G (All-purpose equation solver, Omega Simulation Co. Ltd.) was employed to solve the equations.

5.2 General single reaction mathematical models

5.2.1 Kinetics of the reaction

A typical esterification reaction can be expressed in the following general form.

$$A + B \longleftrightarrow C + H_2O \qquad (5\text{-}11)$$
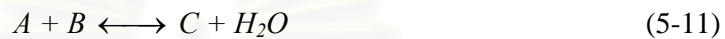
Assuming an elementary reaction, the expression of the reaction rate can be expressed in term of mole fraction as follow:

$$r = Wk(x_A x_B - \frac{x_C x_{H_2O}}{K_{eq}}) \qquad \textbf{(5-12)}$$

5.2.2 Rates of pervaporation

Assuming that partial pressure of all species in the permeate side is low, the permeation rate (Q_i) of species i through the membrane in term of mole fraction can be expressed as:

$$Q_i = AP_i x_i \qquad (5\text{-}13)$$

5.2.3 Modeling of pervaporation membrane reactors

Two modes of continuous pervaporation membrane reactor; i.e. continuous stirred tank (CS-PVMR) and plug flow (PF-PVMR) are considered. The mathematical models were obtained by performing material balances around the reactors. It is assumed that the reactors behave like their ideal reactors. In addition, isothermality, negligible pressure drop, negligible heat- and mass-transfer resistances aside from the permeation process, no coupling effect of mixtures on the permeability were assumed. The sets of equations for different operating modes can be summarized as follows.

$$PF\text{-}PVMR: \qquad \frac{\mathrm{d}}{\mathrm{d}\upsilon}\overline{F}_i = v_i Da\varphi - \frac{Da\delta\, x_i}{\alpha_i} \tag{5-14}$$

$$CS\text{-}PVMR: \qquad \overline{F}_{i,o} - \overline{F}_i + Da\varphi - \frac{Da\delta\, x_i}{\alpha_i} = 0 \tag{5-15}$$

Various design operating parameters and physical property parameters are characterized in dimensionless groups to facilitate parametric analysis for the comparison of reactor performances under different operation modes.

1) Damköhler number, Da $(=kW/F_{A,0})$ is a measure of the residence time,

2) the rate ratio, $(=P_{H_2O}A/kW)$ is a measure of the ratio between permeation rate and reaction rate,

3) the separation factor, $_i$ $(=P_{H_2O}/P_i)$ is a measure of membrane selectivity.

# CHAPTER VI

RESULTS AND DISCUSSIONS

6.1 Pervaporation membrane reactor (PVMR) for the production of methyl acetate

6.1.1 Permeation studies

Table 6.1 summarizes the liquid mole fraction, liquid activity, permeability coefficients and separation factors for the permeation experiments of quaternary mixtures (H_2O-MeOH-HOAc-MeOAc) at 3 temperature levels. It was found that the permeation of acetic acid is negligibly small whereas methanol can permeate through the membrane at significant rate and, hence, the separation factor of methanol, α_{MeOH}, is low. Increasing the temperature results in the decrease of the separation factors. This behavior is observed in many other systems. It should be noted that the expressions shown in terms of activity are more appropriate as the activity deviates significantly from ideality. The obtained permeability coefficients were fitted with good agreement with the Arrhenius equation (shown in Figure 6.1) and the expressions are as follows:

$$P_{H_2O} = 2.01x10^1 \exp(-\frac{3173}{T}) \tag{6-1}$$

$$P_{MeOH} = 2.92 \times 10^5 \exp(-\frac{6756}{T}) \tag{6-2}$$

$$P_{MeOAc} = 7.88 \times 10^7 \exp(-\frac{9385}{T}) \tag{6-3}$$

TABLE 6.1 Feed composition, feed activity, permeability coefficients and separation factor at 3 temperature levels.

Temperature (K)	Liquid Mole Fraction (-)				Liquid Activity (-)				Permeability Coefficient (mol/(m^2.s))				Separation Factor (-)			
	Water	MeOH	MeOAc	HOAc	Water	MeOH	MeOAc	HOAc	Water	MeOH	MeOAc	HOAc	Water	MeOH	MeOAc	HOAc
323	0.1009	0.6748	0.0461	0.1782	0.1720	0.6724	0.0877	0.1672	1.11×10^{-3}	2.33×10^{-4}	1.73×10^{-5}	0	1.0	4.7	64	∞
333	0.1127	0.6617	0.0513	0.1743	0.1916	0.6612	0.0976	0.1670	1.45×10^{-3}	4.79×10^{-4}	5.49×10^{-5}	0	1.0	3.0	26	∞
343	0.1201	0.6378	0.0616	0.1804	0.2055	0.6396	0.1144	0.1758	1.96×10^{-3}	7.88×10^{-4}	9.35×10^{-5}	0	1.0	2.5	21	∞

Figure 6.1 Arrhenius plot of permeability of water/methanol/acetic acid/methyl

acetate mixtures

6.1.2 Pervaporation membrane reactor studies

Figure 6.2 compares the experimental and simulation results of SB-PVMR. The initial moles of HOAc and MeOH were 1 and 5 moles, respectively, and the operating temperature was at $T = 333$ K. The model predicts the experimental results quite well. Discrepancy may be arisen from the deviation of permeability coefficients with compositions due to the interaction between components or from non-ideal behavior in the reactor. However, to simplify the model, this effect was neglected in the study.
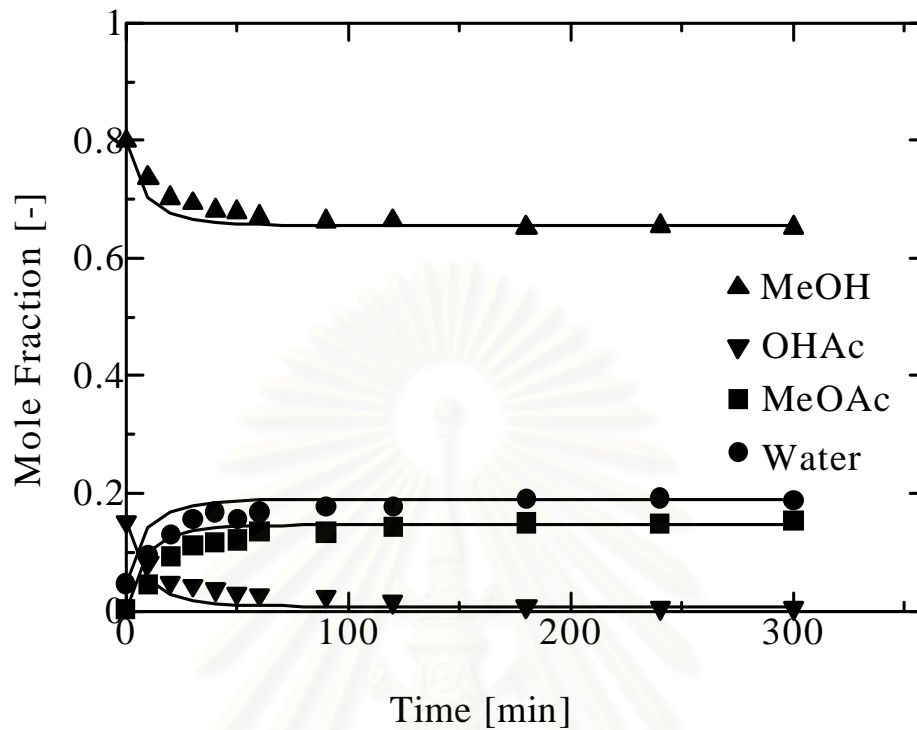
Figure 6.2 Comparison between experimental and simulation results for SB-PVMR
(HOAc:MeOH in mole = 1:5, 15 g of Amberlyst-15, and T = 333 K)

6.1.3 Comparison between two modes of continuous operation

Conversion (X_{HOAc}) is defined as follows.

$$X_{HOAc} = 1 - \frac{(\overline{F}_{HOAc} + \overline{Q}_{HOAc})}{\overline{F}_{HOAc,0}} \tag{6-4}$$

6.1.3.1 Effect of Damköhler number (Da)

Figure 6.3 shows the effect of the Damköhler number (*Da*) on conversion (X_{HOAc}) at various values of the rate ratio (δ). The simulations were based on the values of separation factors (α_i) at T = 323 K and the stoichiometric feed ratio.

Increasing the values of Damköhler number (*Da*) increases residence time and, hence, higher conversions are achieved in both PF-PVMR and CS-PVMR modes. The rate ratio (δ) plays an important role on the performance of PVMR. The case with δ = 0 represents conventional reactors whose maximum conversion is limited at an equilibrium value. At higher value of δ, it is possible to exceed the equilibrium conversion encountered in the conventional reactors. This is in agreement with experimental observations in other systems. Comparing between two operation modes, it is found that PF-PVMR offers higher conversions than CS-PVMR.
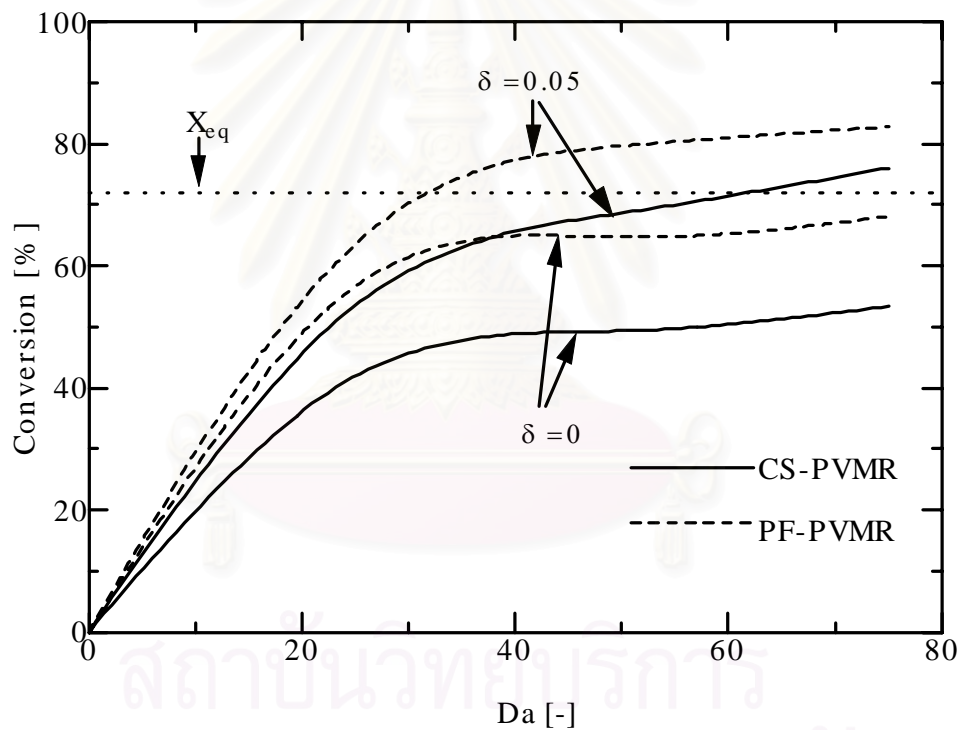
Figure 6.3 Effect of Damköhler number (*Da*) on conversion of HOAc operate in
CS-PVMR and PF-PVMR modes (*T* = 323 K)

6.1.3.2 Effect of rate ratio (δ)

Figures 6.4 and 6.5 show the effect of the rate ratio (δ) at 4 values of Damköhler number (Da = 0.5, 1, 25 and 75). There exists an optimum rate ratio (δ), which provides a maximum conversion, for each value of Damköhler number (Da). Increasing the rate ratio (δ) at its low values is beneficial to the system due to the enhanced forward reaction from the removal of product H_2O; however, the effect of reactant loss retards the improvement at high values of the rate ratio (δ) as shown in Figure 6.5 for Da = 25. The presence of an optimum rate ratio was observed in another system for ethyl acetate production in both PF-PVMR and CS-PVMR modes (Lim *et al*., 2002).

Loss of component in y-axis of Figure 6.6 represents the value of $\overline{Q}_i / \overline{F}_{HOAc,0}$. The superiority among PF-PVMR and CS-PVMR in term of maximum obtainable conversion was obviously dependent on the value of Damköhler number (Da). At low value, CS-PVMR is superior to PF-PVMR; however, the opposite results are observed at higher values. It should be noted that the results reported by Lim *et al*. (2002) only indicate the range where PF-PVMR shows a superior performance than CS-PVMR.

Differences in reactor performances between two operation modes are arisen mainly from the different flow characteristics within the reactors. In CS-PVMR, due to well-mixed condition, the reactant concentrations are at their lowest values and, consequently, the reaction takes place at its lowest rate. However, when considering the separation point of view, the well-mixed condition may be beneficial to the system. Because the product concentrations especially H_2O and the reactant concentrations are at their highest and lowest values, respectively, the entire membrane is efficiently utilized for product removal and, in addition, the reactant losses are at the smallest rates. Considering PF-PVMR, the plug flow condition usually allows the reaction to proceed at higher extent compared to the well-mixed condition due to high reactant concentrations near the reactor entrance; however, it leads to high reactant losses and low product removal at the initial section. In short, the different flow characteristics within the reactors under different operation modes

affect the performance of PVMRs via the effects on the rates of reaction and separation.

At low Damköhler number (Da = 0.5 and 1), CS-PVMR is superior to PF-PVMR. Because the residence time is small, the reaction proceeds at small extent. The effect of H_2O removal on enhancing forward reaction in CS-PVMR is higher than PF-PVMR due to the efficient utilization of membrane area. However, at higher Damköhler number (Da), the increasing reaction rate in PF-PVMR predominates. The reaction moves forward at higher extent and the H_2O removal is high near the end of the reactor. As a result, PF-PVMR is superior to CS-PVMR. It is noted that it is desirable to operate the reactor at high conversion so PF-PVMR seems to be a favorable mode in a practical operation. In addition, the optimum rate ratio (δ) of CS-PVMR is always higher than that of PF-PVMR, indicating that CS-PVMR requires higher membrane area than PF-PVMR.

Figure 6.4 Effect of rate ratio (δ) on conversion of HOAc operate in CS-PVMR and PF-PVMR modes (T = 323 K) at high Da values
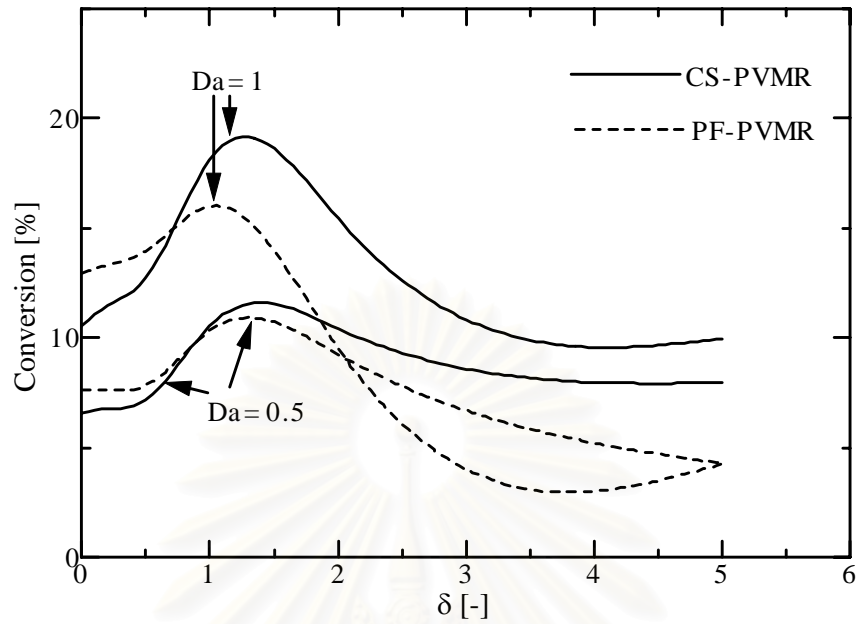
Figure 6.5 Effect of rate ratio (δ) on conversion of HOAc operate in CS-PVMR and PF-PVMR modes ($T = 323$ K) at low Da values
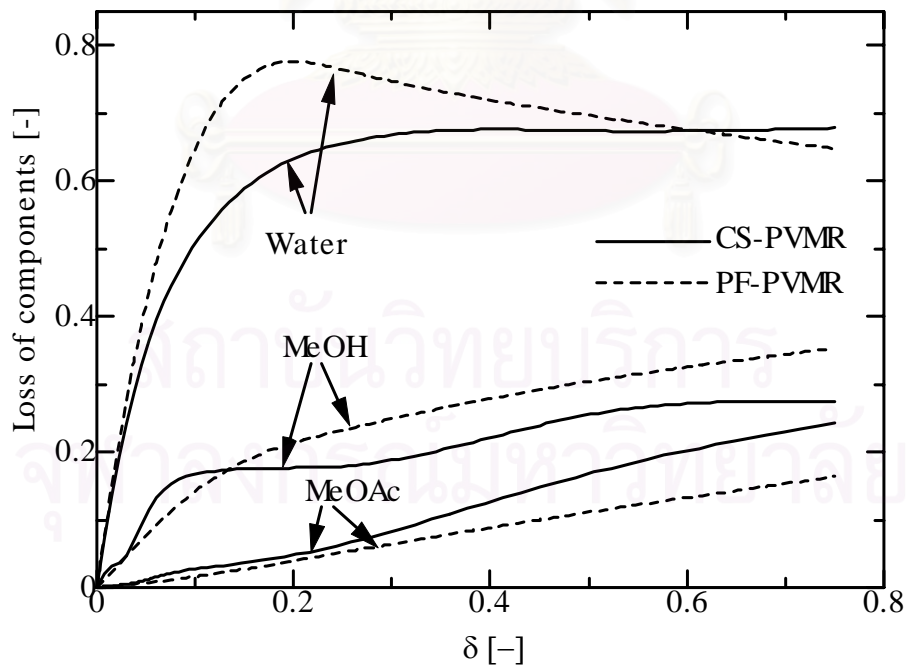
Figure 6.6 Effect of rate ratio (δ) on reactant/product losses for esterification of methyl acetate operate in CS-PVMR and PF-PVMR at $Da = 25$ and $T = 323$ K

6.1.3.3 Effect of feed composition

Since MeOH permeates through the membrane at a significant rate, it is likely to operate the reactor with feed composition of MeOH higher than the stoichiometic value. Figure 6.7 shows the effect of feed composition on the maximum conversion at $Da = 25$ and 75. The maximum conversion was determined by varying the values of the rate ratio (δ) as illustrated in the previous section. It was found that the optimum feed ratio (MeOH/HOAc) is approximately 1.8. Higher feed ratio results in the decreased feed concentration and reaction rate; however, at feed ratio lower than the optimum value, the effect of reactant loss limits the conversion.
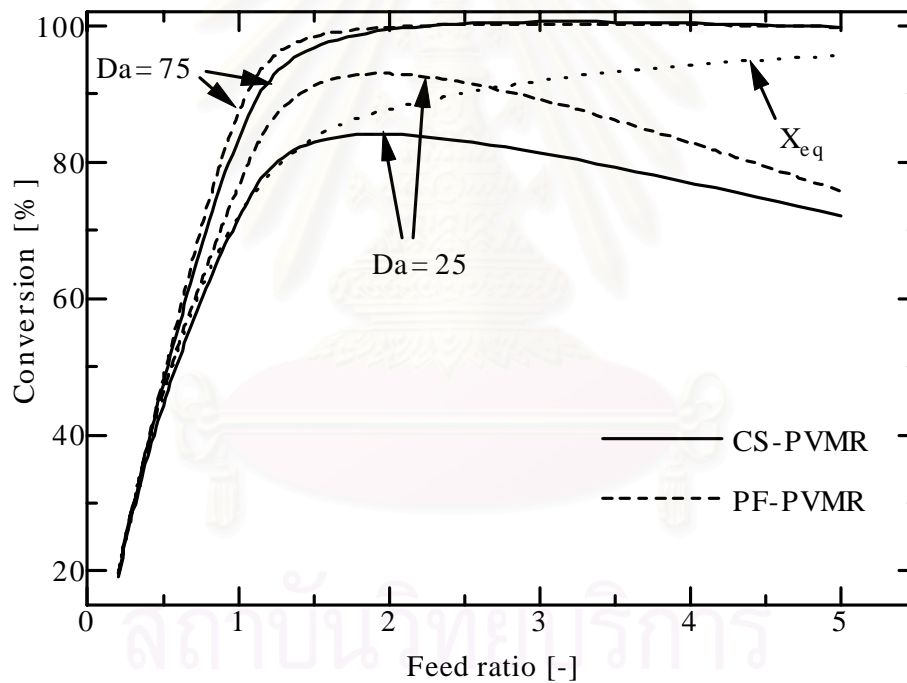
Figure 6.7 Effect of feed composition on conversion of HOAc operate in CS-PVMR and PF-PVMR modes at $\delta = 0.1$ and $T = 323$ K

6.1.3.4 Effect of membrane selectivity

Figure 6.8 shows the effect of membrane selectivity on the conversion for *Da* = 25. ξ is defined as the factor multiplying with the separation factors at *T* = 323 K. The membrane becomes more selective with the increased value of ξ. It is found that for $\xi = 1$, at high values of the rate ratio (δ) the conversion decreases with the increase of the rate ratio (δ) due to the effect of reactant loss (as shown in Figure 6.9). There is no significant improvement when ξ increases from 10 ($\alpha_{MeOH} = 47$) to 100 and 1000 ($\alpha_{MeOH} = 470$ and 4700). Further simulations of PF-PVMR reveals that at $\delta = 0.75$, membranes with $\alpha_{MeOH} = 47$, 141 and 188 are enough to offer the conversions of 95.0, 98.8 and 99.2%, respectively, of that obtained when $\alpha_{MeOH} = 4700$, indicating that there is a range of membrane selectivity which plays an important role on the reactor performance. Again, it is observed that the maximum obtainable conversion of PF-PVMR is superior to that of CS-PVMR at higher membrane selectivity.
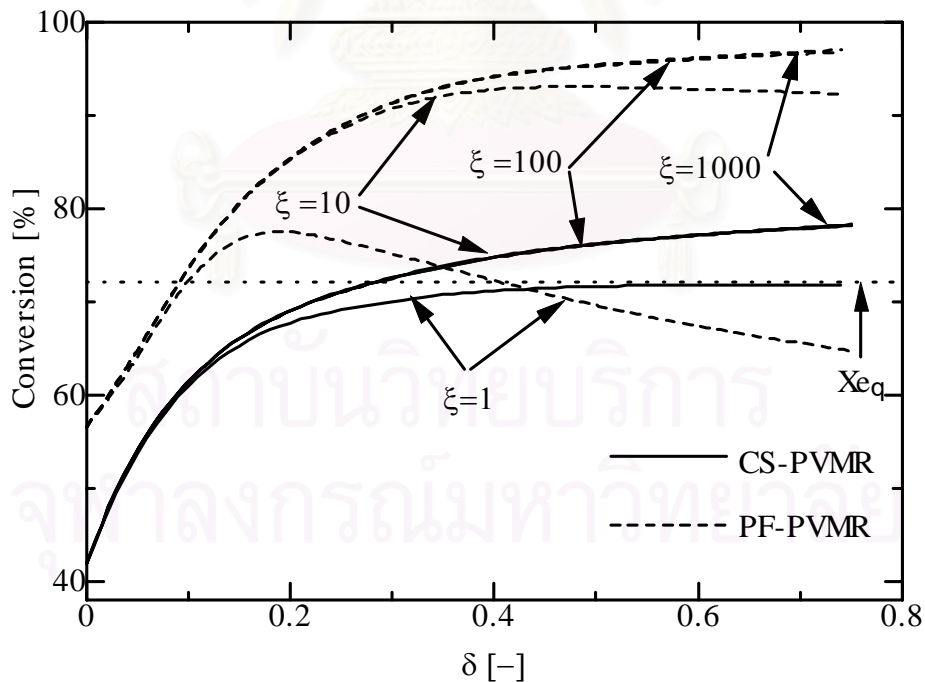
Figure 6.8 Effect of membrane selectivity on conversion of HOAc operate in　CS-PVMR and PF-PVMR mode at *Da* = 25 and *T* = 323 K

Loss of methanol y-axis of Figure 6.9 represents the value of $\overline{Q}_{MeOH} / \overline{F}_{HOAc,0}$. For $\xi = 1$, at high values of the rate ratio (δ) the loss of methanol in PF-PVMR is higher than that in CS-PVMR. However, at higher ξ (=100, 1000), the loss of methanol becomes negligible. Therefore, the selection of pervaporation membrane with higher separation factor of methanol to water is required.
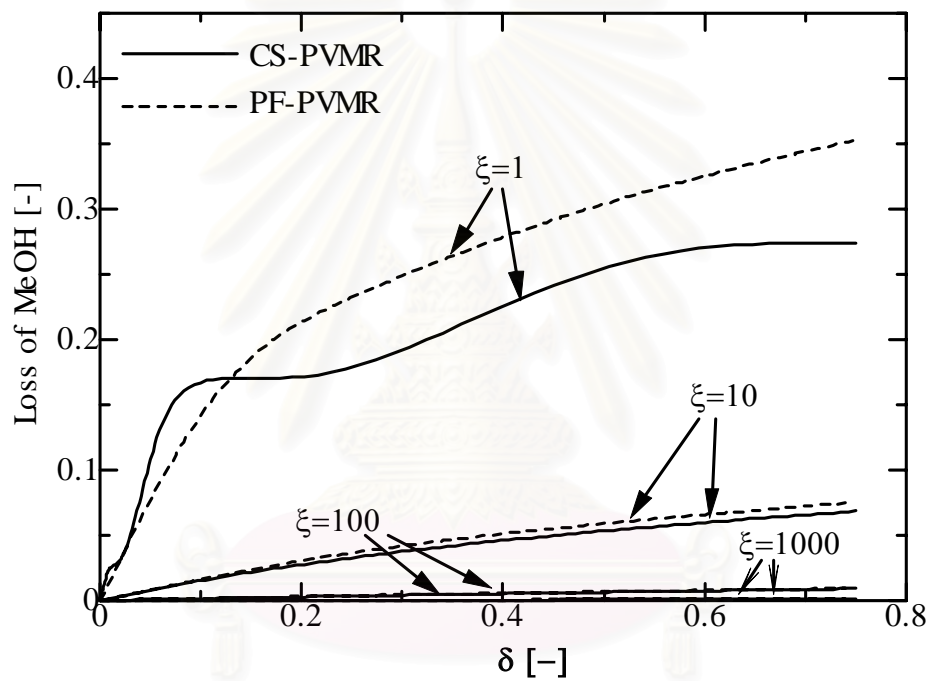
Figure 6.9 Effect of membrane selectivity on MeOH loss operate in CS-PVMR and PF-PVMR mode at $Da = 25$ and $T = 323$ K

6.2 Pervaporation membrane reactor for an esterification reaction expressed in a general form

In this section, the comparisons of the performances between the two modes of PVMRs for an esterification reaction expressed in a general form of $A + B \longleftrightarrow C + H_2O$ are considered. By defining A as a limiting reactant, the conversion (X_A) is defined as follow:

$$X_A = 1 - \frac{(\overline{F}_A + \overline{Q}_A)}{\overline{F}_{A,0}} \tag{6.5}$$

In this general form, the mathematical models and the dimensionless parameters are the same as the previous cases except that the reaction and permeation rates are expressed in terms of mole fraction. The effort is focused on comparing the performances between those modes at different values of the equilibrium constant, K_{eq}. The same values of the membrane selectivity were considered in the studies. Figures 6.10 - 6.12 show the conversion (X_A) of PF-PVMRs at different values of δ and Da when K_{eq} is 0.1, 1.0 and 1,000, respectively. Note that the value of K_{eq} is 0.24 for the simulation study in the previous section. It was found that the effects of Damköhler number (Da) and the rate ratio (δ) follow the same trend as described in the previous case of the methyl acetate production. Compared with the equilibrium conversions of 24.0, 50.0 and 96.9%, respectively, for the cases with $K_{eq} = 0.1$, 1.0 and 1,000, the conversion enhancement is pronounced only at low values of K_{eq}. The differences in conversion between CS-PVMR and PF-PVMR modes are shown in Figures 6.13 – 6.15. The positive values represent the case where CS-PVMR is superior to PF-PVMR. For all values of K_{eq}, this range is observed at relatively high values of δ where the effect of the reactant losses is significant. Considering only the ranges with high degrees of conversion, it was found that the maximum obtainable conversion from PF-PVMR (observed in the range of lower values of δ) is always higher than that from CS-PVMR. It is suggested that PF-PVMR is a favorable mode of operation as long as the operating conditions can be adjusted at a suitable condition. However, if the reactor is operated at relatively high value of δ, CS-PVMR is more suitable for the operation compared to PF-PVMR.
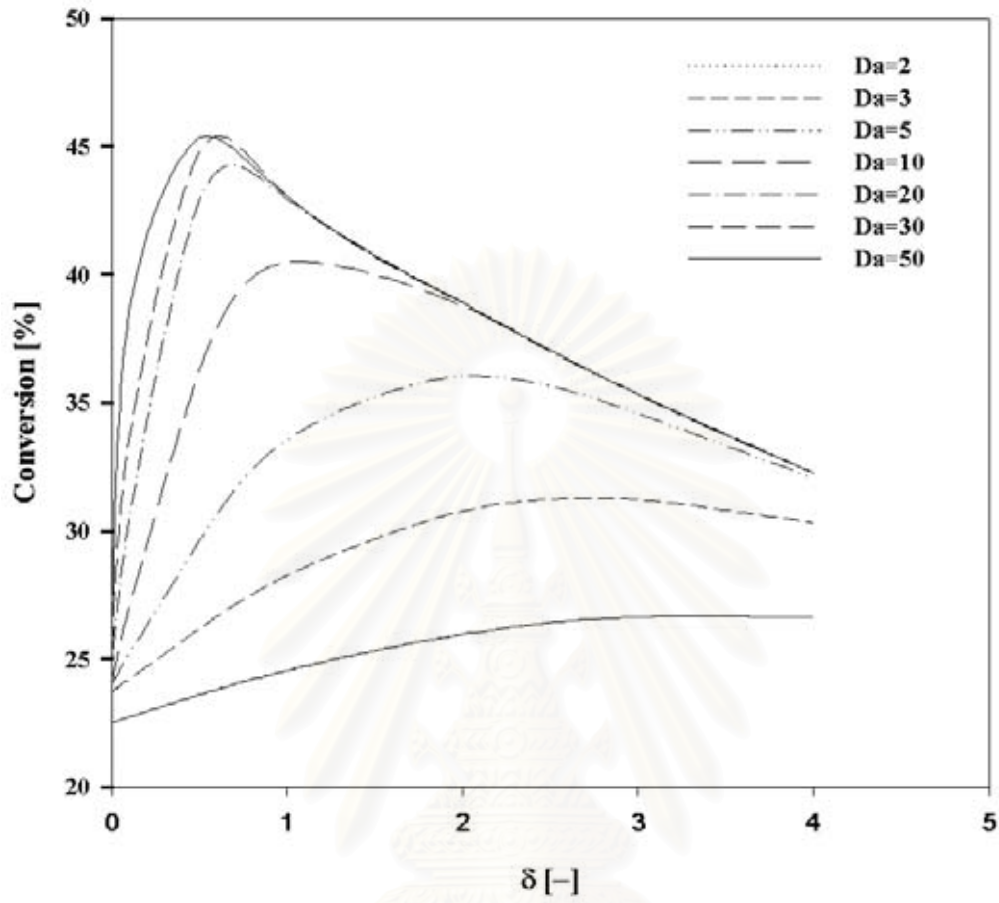
Figure 6.10 Conversion of PF-PVMR at different values of δ and Da

($K_{eq} = 0.1$ and $\alpha_B = 4.7$ and $\alpha_C = 64$)
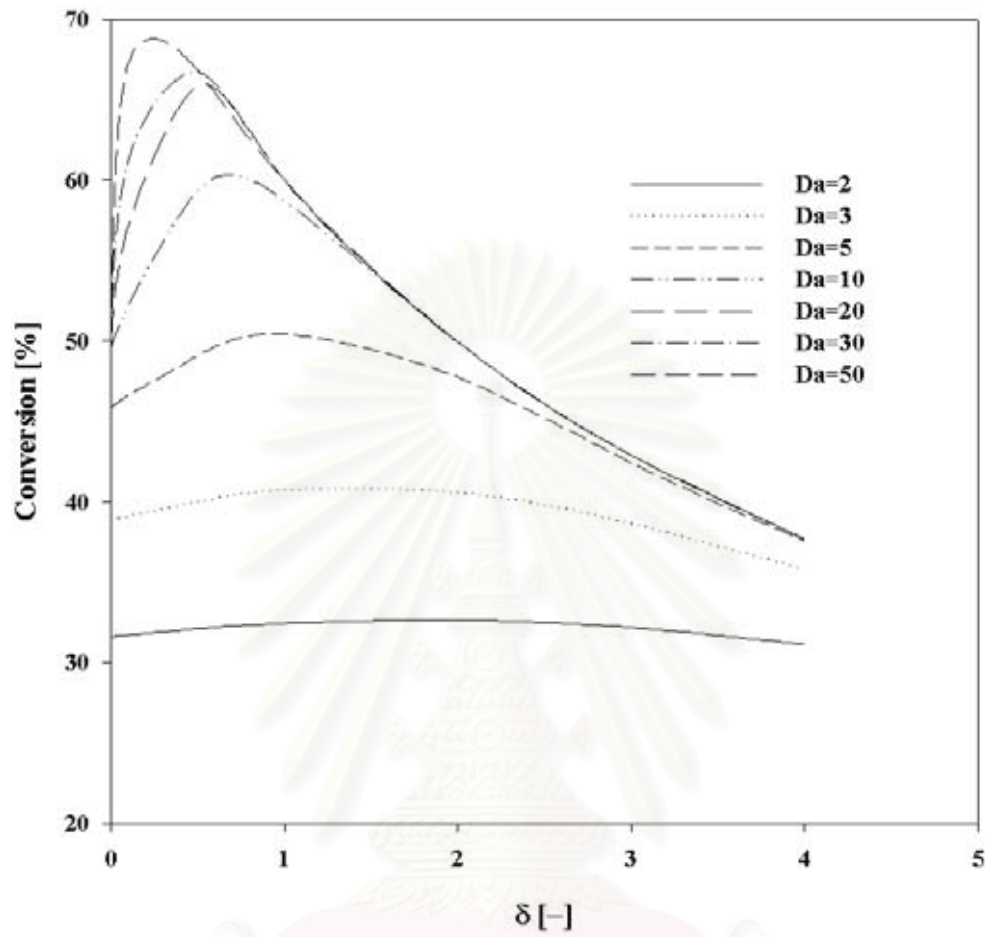
Figure 6.11 Conversion of PF-PVMR at different values of δ and Da

($K_{eq} = 1.0$ and $\alpha_B = 4.7$ and $\alpha_C = 64$)
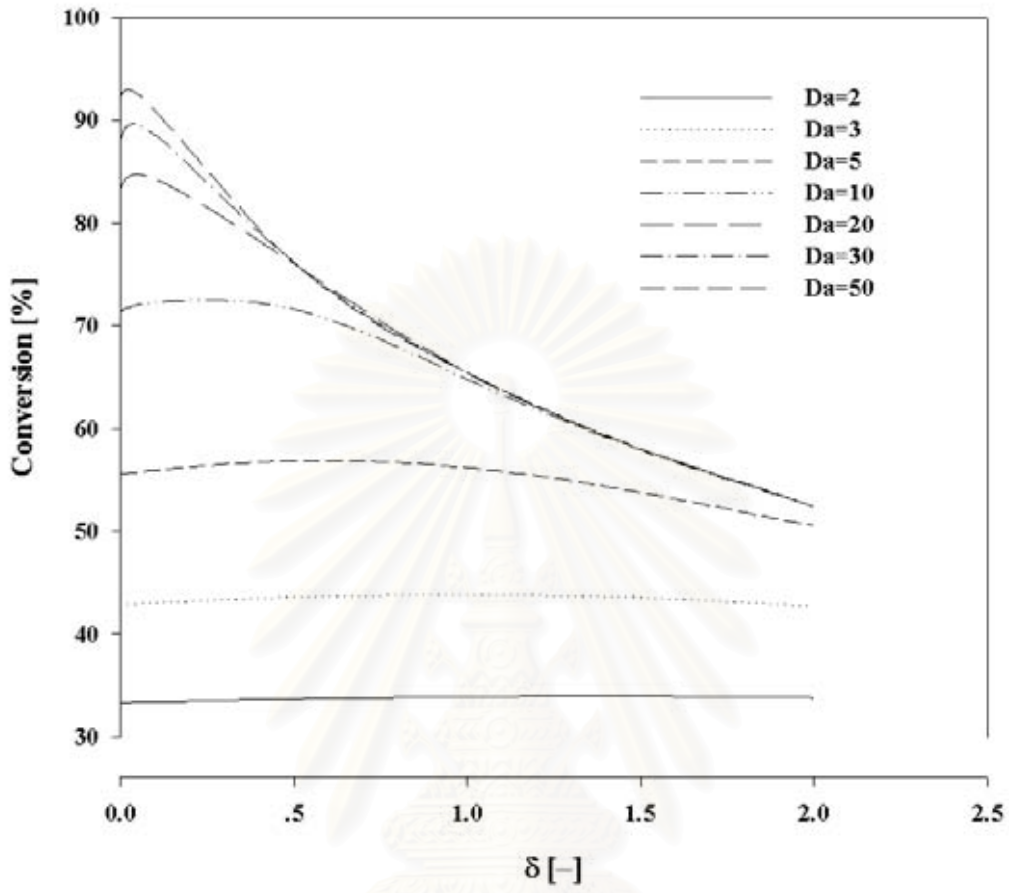
Figure 6.12 Conversion of PF-PVMR at different values of δ and Da

($K_{eq} = 1,000$ and $\alpha_B = 4.7$ and $\alpha_C = 64$)
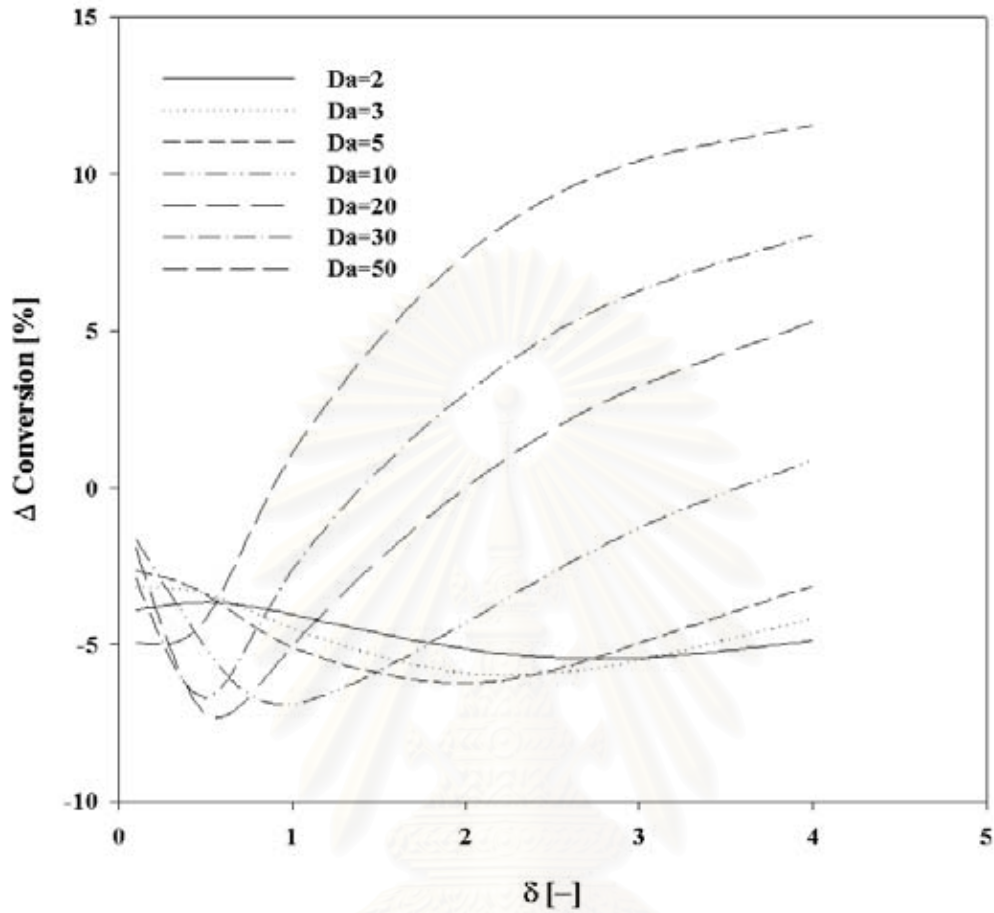
Figure 6.13 Differences of conversion between operation in PF-PVMR and CS-PVMR modes at various Da and δ ($K_{eq} = 0.1$ and $\alpha_B = 4.7$ and $\alpha_C = 64$)
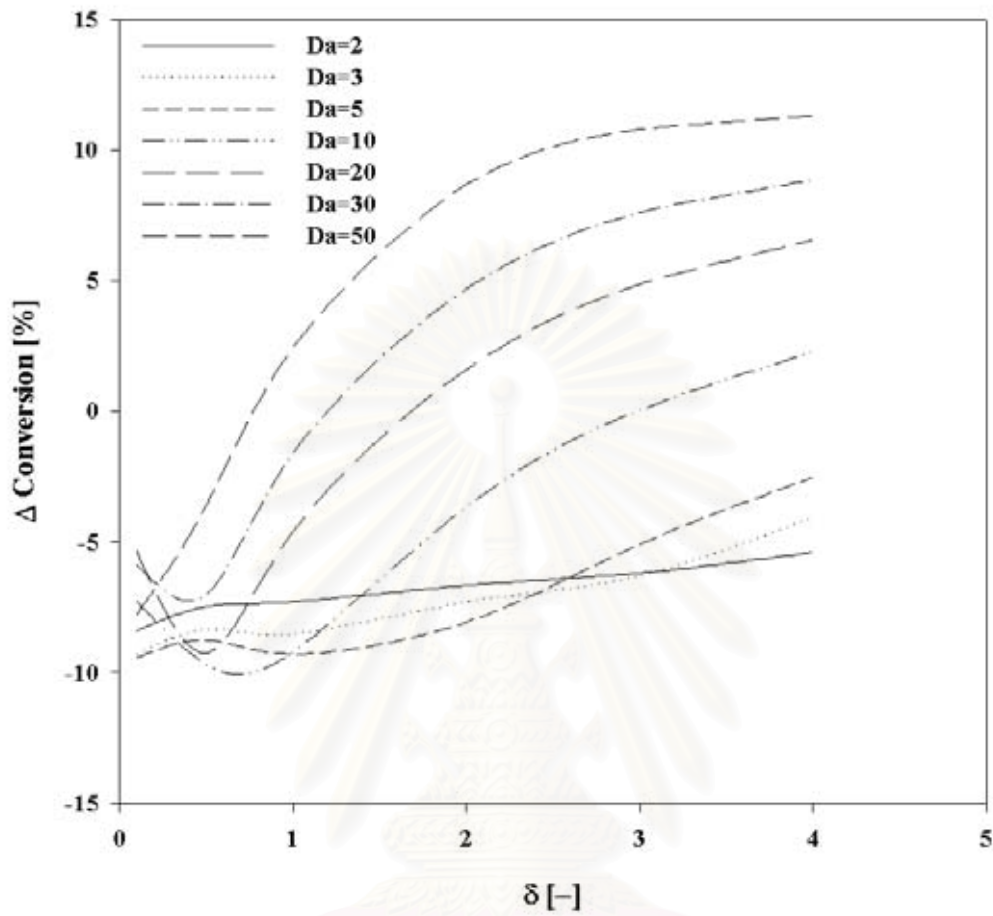
Figure 6.14 Differences of conversion between operation in PF-PVMR and CS-PVMR modes at various Da and δ ($K_{eq} = 1,.0$ and $\alpha_B = 4.7$ and $\alpha_C = 64$)
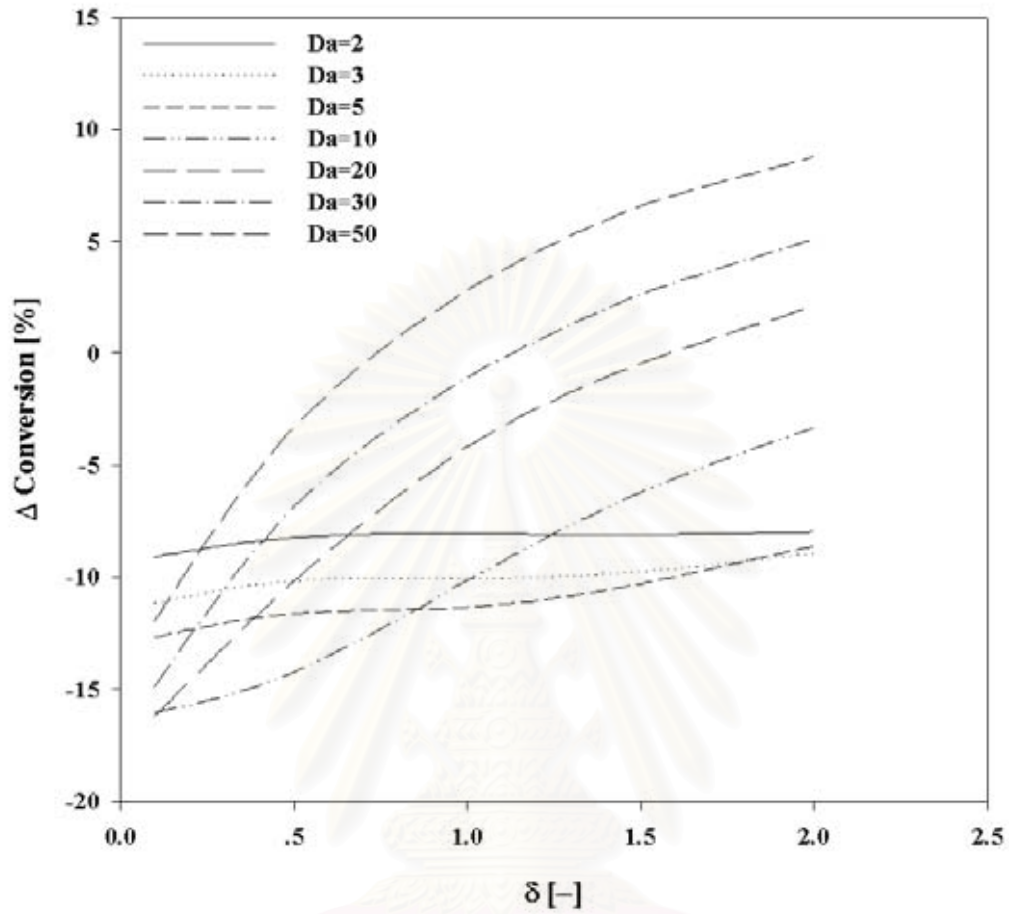
Figure 6.15 Differences of conversion between operation in PF-PVMR and CS-PVMR modes at various Da and δ ($K_{eq} = 1,000$ and $\alpha_B = 4.7$ and $\alpha_C = 64$)

CHAPTER VII

CONCLUSIONS AND RECOMMENDATIONS

7.1 Conclusions

The comparison of performances of pervaporation membrane reactors between two modes of continuous operation; CS-PVMR and PF-PVMR, for the production of methyl acetate from methanol and acetic acid was investigated in the study by using computer simulations. The study was extended to consider a general esterification reaction. The following conclusions can be drawn from the investigations.

7.1.1 Permeation study

The permeation studies of quaternary mixtures of water/methanol/methyl acetate/acetic acid using polyvinyl alcohol (PVA) membrane revealed that the permeation of acetic acid is negligibly small whereas methanol can permeate through the membrane at significant rate and, hence, the separation factor of methanol, α_{MeOH}, was low.

Increasing the temperature results in the decrease of the separation factors.

The obtained permeability coefficients were fitted with good agreement with the Arrhenius equation and the expressions are as follows:

$$P_{H2O} = 2.01 \times 10^1 \exp(-\frac{3173}{T})$$

$$P_{MeOH} = 2.92 \times 10^5 \exp(-\frac{6756}{T})$$

$$P_{MeOAc} = 7.88 \times 10^7 \exp(-\frac{9385}{T})$$

7.1.2 Pervaporation membrane reactor study

The simulation results of SB-PVMR were compared with the experimental results. The model predicted the experimental results quite well. The studies on the continuous PVMRs for the production of methyl acetate showed that

PVMR is able to enhance the conversion higher than at equilibrium value at appropriate operating parameters.

PF-PVMR is a favorable mode although there are some ranges of operating conditions where CS-PVMR is superior to PF-PVMR.

Flow characteristic in the reactor arisen from different mode affects the reactor performance through its influences on the reaction and permeation rates along the reactor.

A membrane with high selectivity is essential for PVMR to achieve high reactor performance.

In addition, the analysis with the general esterification reaction showed that superiority of PVMR compared to conventional reactors is pronounced for the case with low values of K_{eq}. For all levels of K_{eq}, PF-PVMR is a favorable mode of operation as long as the operating conditions can be adjusted at a suitable condition. However, if the reactor is operated at relatively high value of δ, CS-PVMR is more suitable for the operation compared to PF-PVMR.

7.2 Recommendations

This work studies the performance of pervaporation membrane reactor for esterification reaction. The experimental results, however, do not show significant improvement over equilibrium conversion. This is because there is not enough effective membrane area and the driving force by using inert sweep gas may not be sufficient. It is recommended that using a membrane module with high effective

surface area and a vacuum mode as a driving force should be employed to emphasize the improvement of reactor performance from the pervaporation membrane reactor.

The simulations of continuous operation in various configurations such as recycle plug-flow and continuously stirred pervaporation membrane reactor as shown in Fig. 7.1 should be investigated and compared. In addition, in some cases undesired reactions cannot be neglected and, consequently, this more complicated reaction system should be considered.
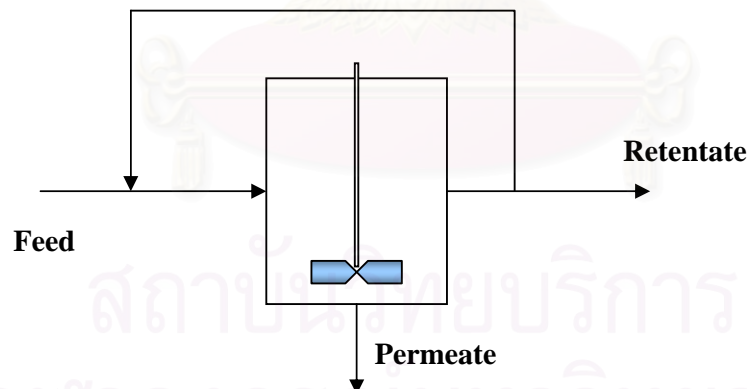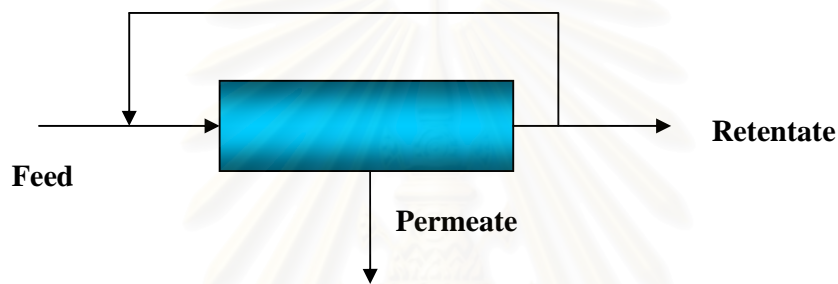
Figure 7.1 Schematic diagrams of pervaporation membrane reactor

(a) recycle plug-flow pervaporation membrane reactor

(b) continuously stirred pervaporation membrane reactor

It is also recommended that other types of multifunctional reactors useful for improving the esterification reactions should be considered. Comparisons on various aspects such as energy consumption should be performed.

REFERENCES

Bengtson, G., H. Scheel, J. Theis, and D. Fritsen. (2002). Catalytic membrane reactor to simultaneously concentrate and react organics. **Chemical Engineering Journal** 85: 303-311.

Bernal, M. P., J. Coronas, M. Menéndez, and J. Santamaría. (2002). Coupling of reaction at the microscopic level: esterification processes in a H-ZSM-5 membrane reactor. **Chemical Engineering Science** 57: 1557-1562.

David, M. O., T. Q. Nguyen, and J. Neel. (1991). Pervaporation-esterification coupling: Part I Basic kinetic model. **Chem. Eng. Res. Des.** 69: 335-340.

David, M. O., T.Q. Nguyen, J. Neel. (1991). Pervaporation-esterification coupling: Part II Modelling of the influence of different operating parameters. **Chem. Eng. Res. Des.** 69: 341-346.

Domingues, L., F. Recasens, and M. A. Larrayoz. (1999). Studies of a pervaporation reactor: kinetics and equilibrium shift in benzyl alcohol acetylation. **Chemical Engineering Science** 54: 1461-1465.

Feng, X., and R. T. M. Huang. (1996). Studies of a membrane reactor: esterification facilitated by pervaporation. **Chemical Engineering Science** 51: 4673-4679.

Feng, X., and R. Y. M. Huang. (1997). Liquid separation by membrane pervaporation: a review. **Ind. Eng. Chem. Res.** 36: 1048-1066.

Huang, R.Y.M. (1991). Pervaporation membrane separation processes. Netherland: Elsevier Science Publishers B.V.

Jennings, J. F., and R. C. Binning. (1960). Removal of water generated in organic chemical reactions. US Patent, 2,956,070.

Keurentjes, J. T. F., G. H. R. Janssen, and J. J. Gorissen. (1994). The esterification of tartaric acid with ethanol: kinetics and shifting the equilibrium by means of pervaporation. **Chemical Engineering Science** 49: 4681-4689.

Kiatkittipong, W., S. Assabumrungrat, and P. Praserthdam. (2002a). Synthesis of ethyl tert-Butyl ether from tert-Butyl alcohol and ethanol catalyzed by β-zeolite in pervaporation membrane reactors. **J. of The Institution of Engineering Singapore** 42: 6-10.

Kiatkittipong, W., S. Assabumrungrat, P. Praserthdam, and S. Goto. (2002b). A pervaporation membrane reactor for liquid phase Synthesis of ethyl tert-Butyl ether from tert-Butyl alcohol and ethanol. **J. of Chemical Engineering of Japan** 35: 547-556.

Kita, H., K. Tanaka, K. I. Okamoto, and M. Yamamoto. (1987). The esterification of oleic acid with ethanol accompanied by membrane separation. **Chemical Letter** 2053-2056.

Kita, H., S. Sasaki, K. Tanaka, K. I. Okamoto, and M. Yamamoto. (1988). Esterification of carboxylic acid with ethanol accompanied by membrane separation. **Chemical Letter** 2025-2028.

Krupiczka, R., and Z. Koszorz. (1999). Activity-based model of the hybrid process of an esterification reaction coupled with pervaporation. **Separation and Purification Technology** 16: 55-59.

Lim, S. Y., B. Park, F. Hung, M. Sahimi, and T. T. Tsotsis (2002). Design issues of pervaporation membrane reactors for esterification. **Chemical Engineering Science** 57: 4933-4946.

Lipnizki, F., R. W. Field, and P. K. Ten (1999). Pervaporation based hybrid process: a review of process design, application and economics. **J. of Membrane Science** 153: 183-210.

Liu, Q. L., Z. Zhang, and H. F. Chen. (2001). Study on the coupling of esterification with pervaporation. **J. of Membrane Science** 182: 173-181.

Liu, Q. L., and H. F. Chen. (2002). Modeling of esterification of acetic acid with n-butanol in the presence of $Zr(SO_4)_2 4H_2O$ coupled pervaporation. **J. of Membrane Science** 196: 171-178.

Lizon, T. G., E. Edwards, G. Lobiundo, and L. F. D. Santos (2002). Dehydration of water/t-butanol mixtures by pervaporation: comparative study of commercially available polymeric, microporous silica and zeolite membranes. **J. of Membrane Science** 197: 309-319.

Marcano, J. G. S., and Th. T. Tsotsis. (2002). Catalytic membrane and membrane reactors. Federal Republic of Germany: WILEY-VCH Verlag Gmbh.

Nunes, S. P., and K. V. Peinemann. (2001). Membrane technology in the chemical industry. Federal Republic of Germany: WILEY-VCH Verlag Gmbh.

Okamoto, K. I., M. Yamamoto, Y. Otoshi, T. Semoto, M. Yono, K. Tanaka, and H. Kita. (1993). Pervaporation-aided esterification of oleic acid. **J. of Chemical Engineering of Japan** 26: 475-481.

Popken, T., L. Gotze, J. Gmehling. (2000). Reaction kinetics and chemical equilibrium of homogeneously and heterogeneously catalyzed acetic acid esterification with methanol and methyl acetate hydrolysis. **Ind. Eng. Chem. Res.** 39: 2601-2611.

Tanaka, K., R. Yoshikawa, C. Ying, H. Kita, and K. I. Okamoto. (2001). Application of zeolite membranes to esterification reactions. **Catalysis today** 67: 121-125.

Timashev S. F., V. V. Valuev, R. R. Salem, and A. G. Strugatshaga. (1994). Pervaporation induced by electric current. **J. of Membrane Science** 91: 249-258.

Waldburger, R., F. Widmer, and W. Heinzelmann. (1994). Combination of esterification and Pervaporation in a continuous Membrane reactor. **Chem. Ing. Tech.** 66: 850-854.

Wijmans, J. G., and R. W. Baker. (1995). The solution-diffusion model: a review. **J. of Membrane Science** 107: 1-21.

Xuehui, L., and W. Lefu. (2001). Kinetic model for an esterification process coupled by pervaporation. **J. of Membrane Science** 186: 19-24.

Zhu, Y., G. Minet, and T. T. Tsotsis. (1996). A continuous pervaporation membrane reactor for the study of esterification reactions using composite polymeric/ceramic membrane. **Chemical Engineering Science** 51: 4103-4113.

Zhu, Y., and H. Chen (1998). Pervaporation separation and pervaporation-esterification coupling using crosslinked PVA composite catalytic membranes on porous ceramic plate. **J. of Membrane Science** 138: 123-134.

APPENDICES

APPENDIX A

MATHEMATICAL MODELS

This appendix concerns the development of mathematical models for three modes of pervaporation membrane reactors It is assumed that apart from the main esterification reaction ($A + B \longleftrightarrow C + H_2O$) there is no other side reaction in the system. The expressions of reaction rate and permeation rate can be expressed as shown in Equations (4-2) and (4-3) in Chapter IV. It is noted that the partial pressure of component i in the permeation side is assumed negligible. The mathematical models were derived by performing material balances around the reactors. The followings are details for each type of PVMR mode.

1. Semi-Batch Pervaporation Membrane Reactor (SB-PVMR)
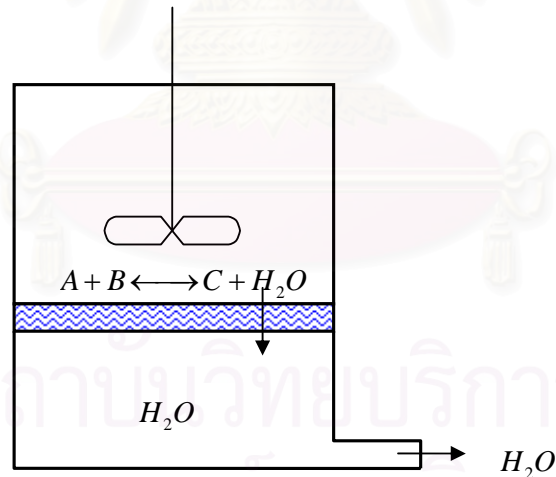
Figure A.1 schematic diagram of a semi-batch pervaporation membrane reactor

Figure A.1 shows schematic diagram of a semi-batch pervaporation membrane reactor. It is assumed that the reaction mixture is well-mixed and permeation through a membrane is in quasi-steady state. The material balance for the reaction side is

Rate of accumulation = rate of generation – rate of permeation

$$\frac{dN_i}{dt} = v_i w k \left(x_A x_B - \frac{x_C x_{H_2O}}{K_{eq}} \right) - A P_i x_i \qquad \text{(A-1)}$$

2. Continuously-Stirred Pervaporation Membrane Reactor (CS-PVMR)

A, B $\longrightarrow$ C

$A + B \longleftrightarrow C + H_2O$

H_2O

H_2O
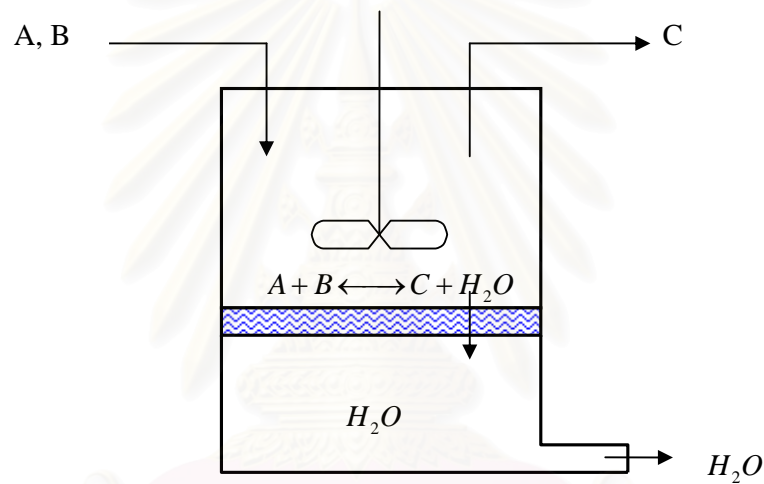
Figure A.2 schematic diagram of a continuously-stirred pervaporation membrane reactor

Figure A.2 shows the schematic diagram of a continuously-stirred pervaporation membrane reactor. The following assumptions were proposed for developing the mathematical model of CS-PVMR.

1. The reactor is operated at steady-state condition and behaves as an ideal CSTR.

2. The concentration polarization effect on the reaction side is considered negligible.

3. The permeation through a membrane is at quasi-steady state.

By performing the material balance around the reaction side, the following equation can be obtained.

Rate of accumulation = rate of mass in – rate of mass out + rate of generation – rate of permeation

$$0 = F_{i,0} - F_i + v_i wk\varphi - AP_i x_i \tag{A-2}$$

where

$$\varphi = \left(x_A x_B - \frac{x_C x_{H_2O}}{K_{eq}} \right)$$

By defining the following dimensionless groups:

$$Da = \frac{kW}{F_{A,0}}, \qquad \delta = \frac{P_{H_2O} A}{kW}, \qquad \alpha_i = \frac{P_{H_2O}}{P_i},$$

$$\overline{F}_{i,0} = \frac{F_{i,0}}{F_{A,0}}, \qquad \overline{F}_i = \frac{F_i}{F_{A,0}}$$

the above equation can be written in a dimensionless form as follows:

$$\overline{F}_{i,0} - \overline{F}_i + v_i Da\varphi - \frac{Da\delta \, x_i}{\alpha_i} = 0 \tag{A-3}$$

3. Plug Flow Pervaporation Membrane Reactor (PF-PVMR)
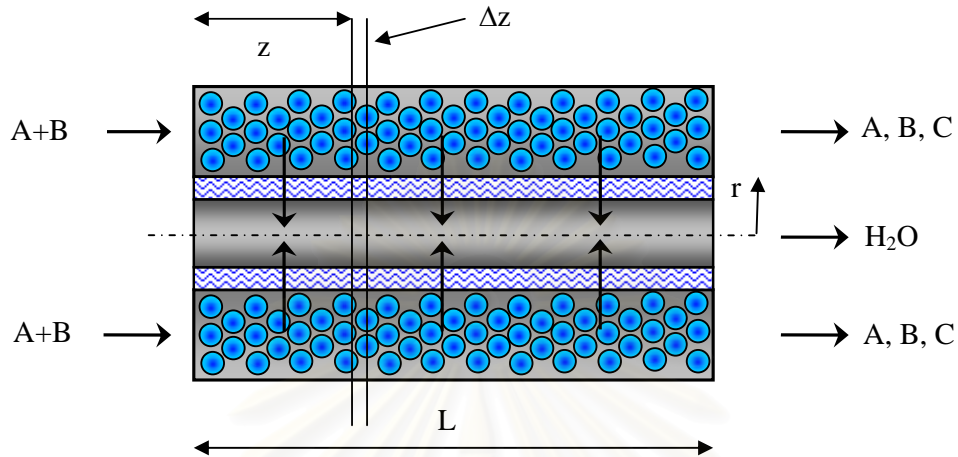
Figure A.3 schematic diagram of a plug flow pervaporation membrane reactor

The additional assumptions applied for the PF-PVMR mathematical model are as follows:

      1. The reactor is operated at steady-state condition and behaves as an ideal PFR.

      2. The concentration polarization effect on the reaction side is considered negligible.

By performing the material balance around a small element ΔZ.

Rate of accumulation = rate of mass in – rate of mass out + rate of generation – rate of permeation

$$F_i l_z - F_i l_{z+\Delta z} + v_i \rho \, \pi \, r^2 \Delta z k \varphi - 2\pi r \Delta z P_i x_i = 0 \tag{A-4}$$

Taking limit Δz to 0 of (A-4)

$$\frac{dF_i}{dz} = v_i \rho \, \pi \, r^2 k \, \varphi - 2\pi \, r P_i x_i \tag{A-5}$$

Dividing (A-13) with πr^2 as

$$\frac{dF_i}{dV} = v_i \rho \, k \, \varphi - \frac{2P_i x_i}{r} \tag{A-6}$$

rearrange (A-6) into dimensionless form as:

$$\frac{dF_i}{d\upsilon} = v_i k W \varphi - P_i A x_i \tag{A-7}$$

By defining the following dimensionless groups:

$$Da = \frac{kW}{F_{A,0}}, \qquad \delta = \frac{P_{H_2O} A}{kW}, \qquad \alpha_i = \frac{P_{H_2O}}{P_i},$$

$$\overline{F}_{i,0} = \frac{F_{i,0}}{F_{A,0}}, \qquad \overline{F}_i = \frac{F_i}{F_{A,0}}$$

the above equation can be expressed in a dimensionless form as follow.

$$\frac{d\overline{F}_i}{d\upsilon} = v_i Da \varphi - \frac{Da \delta \, x_i}{\alpha_i} \tag{A-8}$$

APPENDIX B

UNIFAC METHOD

The UNIFAC method for estimation of activity coefficient depends on the concept that a liquid mixture may be considered as a solution of the structural units from which the molecules are formed rather than a solution of the molecules themselves. These structural units are called subgroups, and some of them are listed in the second column of   Table B-1. A number, designated k, identifies each subgroup. The relative volume R_k and relative surface area Q_k are properties of the subgroups, and values are listed in column 4 and 5 of Table B.1. When it is possible to construct a molecule from more than one set of subgroups, the set containing the least member of different subgroups is the correct set. The great advantage of the UNIFAC method is that a relatively small number of subgroups combine to form a very large number of molecules.

Activity coefficients depend not only on the subgroup properties R_k and Q_k, but also on interactions between subgroups. Here, similar subgroups are assigned to a main group, as shown in the first two columns of Table B.1. The designations of main groups, such as "CH_2", "ACH", etc., are descriptive only. All subgroups belonging to the same main group are considered identical with respect to group interactions. Therefore parameters characterizing group interactions are identified with pairs of main groups. Parameter value a_{mk} for a few such pairs are given in Table B.2.

The UNIFAC method is based on the UNIQUAC equation which treats $g \equiv G^E / RT$ as comprised of two additive parts, a *combinatorial* term g^C to account for molecular size and shape differences, and a *residual* term g^R to account for molecular interactions:

$$g = g^C + g^R \qquad\qquad\qquad (\text{B-1})$$

Function g^C contains pure-species parameters only, whereas function g^R incorporates two binary parameters for each pair of molecules. For a multi-component system,

$$g^C = \sum x_i \ln \frac{\phi_i}{x_i} + 5 \sum q_i x_i \ln \frac{\theta_i}{\phi_i} \tag{B-2}$$

and

$$g^R = -\sum q_i x_i \ln(\sum \theta_j \tau_{ji}) \tag{B-3}$$

where

$$\phi_i = \frac{x_i r_i}{x_j r_{j_i}} \tag{B-4}$$

and

$$\theta_i = \frac{x_i q_i}{x_j q_{j_i}} \tag{B-5}$$

Subscript i identifies species, and j is a dummy index; all summations are over all species. Note that $\tau_{ji} \neq \tau_{ii}$; however, when $i = j$, then $\tau_{jj} = \tau_{ii} = 1$. In these equations r_i (a relative molecular volume) and q_i (a relative molecular surface area) are pure-species parameters. The influence of temperature on g enters through the interaction parameters τ_{ji} of Equation (B-3), which are temperature dependent:

$$\tau_{ji} = \exp \frac{-(u_{ji} - u_{ii})}{RT} \tag{B-6}$$

Parameters for the UNIQUAC equation are therefore values of $(u_{ji} - u_{ii})$.

An expression for $\ln \gamma_i$ is applied to the UNIQUAC equation for g [Equation (B-1) through (B-3)]. The result is given by the following equations:

$$\ln \gamma_i = \ln \gamma_i^C + \ln \gamma_i^R \tag{B-7}$$

$$\ln \gamma_i^C = 1 - J_i + \ln J_i - 5q_i(1 - \frac{J_i}{L_i} + \ln \frac{J_i}{L_i}) \tag{B-8}$$

and

$$\ln \gamma_i{}^R = q_i(1 - \ln s_i - \sum_j \theta_j \frac{\tau_{ij}}{s_j}) \qquad \text{(B-9)}$$

where in addition to Equations (B-5) and (B-6)

$$J_i = \frac{r_i}{\sum x_j r_j} S \qquad \text{(B-10)}$$

$$L_i = \frac{q_i}{\sum x_j q_j} S \qquad \text{(B-11)}$$

$$s_i = \sum \theta_l \tau_{li} \qquad \text{(B-12)}$$

Again subscript i identifies species, and j and l are dummy indices. All summations are over all species, and $\tau_{ij} = 1$ for $i=j$. Values for the parameters ($u_{ij} - u_{jj}$) are found by regression of binary VLE data.

When applied to a solution of groups, the activity coefficients are calculated by:

$$\ln \gamma_i = \ln \gamma_i^C + \ln \gamma_i^R \qquad \text{(B-13)}$$

when

$$\ln \gamma_i^C = 1 - J_i + \ln J_i - 5 q_i (1 - \frac{J_i}{L_i} + \ln \frac{J_i}{L_i}) \qquad \text{(B-14)}$$

and

$$\ln \gamma_i^R = q_i [1 - (\theta_k \frac{\beta_{ik}}{s_k} - e_{ki} \ln \frac{\beta_{ik}}{s_k})] \qquad \text{(B-15)}$$

The quantities J_i and L_i are given by:

$$J_i = \frac{r_i}{x_j r_j} \tag{B-16}$$

$$L_i = \frac{q_i}{x_j q_j} \tag{B-17}$$

In addition, the following definition of parameters in Equation B-14 and B-15 apply:

$$r_i = v_k^{(i)} R_k \tag{B-18}$$

$$q_i = v_k^{(i)} Q_k \tag{B-19}$$

$$e_{ki} = \frac{v_k^{(i)} Q_k}{q_i} \tag{B-20}$$

$$\beta_{ik} = e_{mi} \tau_{mk} \tag{B-21}$$

$$\theta_{ik} = \frac{x_i q_i e_{ki}}{x_j q_j} \tag{B-22}$$

$$s_k = \theta_m \tau_{mk} \tag{B-23}$$

$$\tau_{mk} = \exp(\frac{-a_{mk}}{T}) \tag{B-24}$$

Subscript i identifies species, and j is a dummy index running over all species. Subscript k identifies subgroups, and m is a dummy index running over all subgroups. The quantity $v_k^{(i)}$ is the number of subgroups of type k in a molecule of species i. Values of the subgroup parameters R_k and Q_k and of the group interaction parameters, a_{mk} come from tabulation in the literature. Tables B.1 and B.2 show some parameter values.

TABLE B.1: UNIFAC-VLE subgroup parameters[†]

Main group	Subgroup	Group name	Rk	Qk
1	1	CH_3	0.9011	0.848
1	2	CH_2	0.6744	0.540
1	3	CH	0.4469	0.228
1	4	C	0.2195	0.000
2	5	$CH_2=CH$	1.3454	1.176
2	6	CH=CH	1.1167	0.867
2	7	$CH_2=C$	1.1173	0.988
2	8	CH=C	0.8886	0.676
2	9	C=C	0.6605	0.485
3	10	ACH	0.5313	0.400
3	11	AC	0.3652	0.120
4	12	$ACCH_3$	1.2663	0.968
4	13	$ACCH_2$	1.0396	0.660
4	14	ACCH	0.8121	0.348
5	15	OH	1.0000	1.200
6	16	CH_3OH	1.4311	1.432
7	17	H2O	0.9200	1.400
8	18	ACOH	0.8952	0.680
9	19	CH_3CO	1.6724	1.488
9	20	CH_2CO	1.4457	1.180
10	21	CHO	0.9980	0.948
11	22	CH_3COO	1.9031	1.728
11	23	CH_2COO	1.6764	1.420
12	24	HCOO	1.2420	1.188
13	25	CH_3O	1.1450	1.088
13	26	CH_2O	0.9183	0.780
13	27	CH-O	0.6908	0.468
13	28	FCH_2O	0.9183	1.100
14	29	CH_3NH_2	1.5959	1.544
14	30	CH_2NH_2	1.3692	1.236
14	31	$CHNH_2$	1.1417	0.924
15	32	CH_3NH	1.4337	1.244
15	33	CH_2NH	1.2070	0.936
15	34	CHNH	0.9795	0.624
16	35	CH_3N	1.1865	0.940
16	36	CH_2N	0.9597	0.632
17	37	$ACNH_2$	1.0600	0.816
18	38	C_5H_5N	2.9993	2.113
18	39	C_5H_4N	2.8332	1.833
18	40	C_5H_3N	2.6670	1.553
19	41	CH_3CN	1.8701	1.724
19	42	CH_2CN	1.6434	1.416
20	43	COOH	1.3013	1.224
20	44	HCOOH	1.5280	1.532
21	45	CH_2Cl	1.4654	1.264
21	46	CHCl	1.2380	0.952
21	47	CCl	1.0060	0.724

TABLE B.2: UNIFAC-VLE Group Interaction Parameters, a_{mk}, in kelvins[†]

a_{mk} m	k Name	1 CH$_2$	2 C=C	3 ACH	4 ACCH$_2$	5 OH	6 CH$_3$OH	7 H$_2$O	8 ACOH	9 CH$_2$CO	10 CHO	11 CCOO	12 HCOO	13 CH$_2$O	14 CNH$_2$	15 CNH$_2$	16 (C)$_3$N	17 ACNH$_2$	18 PYRIDINE	19 CCN	20 COOH
1	CH$_2$	0	86.02	61.13	76.5	986.5	697.2	1318	1333	476.4	677	232.1	741.4	251.5	391.5	225.7	206.6	920.7	287.7	597	663.5
2	C=C	-35.36	0	38.81	74.15	524.1	787.6	270.6	526.1	182.6	448.8	37.85	449.1	214.5	240.9	163.9	61.11	749.3	0	336.9	318.9
3	ACH	-11.12	3.446	0	167	636.1	637.3	903.8	1329	25.77	347.3	5.994	-92.55	32.14	161.7	122.8	90.49	648.2	-4.449	212.5	537.4
4	ACCH$_2$	-69.7	-113.6	-146.8	0	803.2	603.2	5695	884.9	-52.1	586.6	5688	115.2	213.1	0	-49.29	23.5	664.2	52.8	6096	603.8
5	OH	156.4	457	89.6	25.82	0	-137.1	353.5	-259.7	84	441.8	101.1	193.1	28.06	83.02	42.7	-323	-52.39	170	6.712	199
6	CH$_3$OH	16.51	-12.52	-50	-44.5	249.1	0	-181	-101.7	23.39	306.4	-10.72	193.4	-128.6	359.3	266	53.9	489.7	580.5	36.23	-289.5
7	H$_2$O	300	496.1	362.3	377.6	-229.1	289.6	0	324.5	-195.4	-257.3	72.87	0	540.5	48.89	168	304	-52.29	459	112.6	-14.09
8	ACOH	275.8	217.5	25.34	244.2	-451.6	-265.2	-601.8	0	-356.1	0	-449.4	0	0	0	0	0	119.9	-305.5	0	0
9	CH$_2$CO	26.76	42.92	140.1	365.8	164.5	108.7	472.5	-133.1	0	-37.36	-213.7	-38.47	-103.6	0	0	-169	6201	165.1	481.7	669.4
10	CHO	505.7	56.3	23.39	106	-404.8	-340.2	232.7	0	128	0	-110.3	11.31	304.1	0	0	0	0	0	0	0
11	CCOO	114.8	132.1	85.84	-170	245.4	249.6	200.8	-36.72	372.2	185.1	0	372.9	-235.7	0	-73.5	0	475.5	0	494.6	660.2
12	HCOO	90.49	-62.55	1967	2347	191.2	155.7	0	0	70.42	35.35	-261.1	0	0	0	0	0	0	0	0	-356.3
13	CH$_2$O	83.36	26.51	52.13	65.69	237.7	238.4	-314.7	0	191.1	-7.838	461.3	0	0	141.7	0	0	0	0	-18.51	664.6
14	CNH$_2$	-30.48	1.163	-44.85	0	-164	-481.7	-330.4	0	0	0	0	0	0	0	63.72	-41.11	-200.7	0	0	0
15	CNH$_2$	65.33	-28.7	-22.31	223	-150	-500.4	-448.2	0	0	0	136	0	-49.3	108.8	0	-189.2	0	0	0	0
16	(C)$_3$N	-83.98	-25.38	-223.9	109.9	28.6	-406.8	-598.8	0	225.3	0	0	0	0	38.89	865.9	0	0	0	0	0
17	ACNH$_2$	1139	2000	247.5	762.8	-17.4	-118.1	-367.8	-253.1	-450.3	0	-294.8	0	0	-15.07	0	0	0	0	-281.6	0
18	PYRIDINE	-101.6	0	31.87	49.8	-132.3	-378.2	-332.9	-341.6	-51.54	0	0	0	0	0	0	0	0	0	-169.7	-153.7
19	CCN	24.82	-40.62	-22.97	-138.4	-185.4	157.8	242.8	0	-287.5	0	-266.6	0	38.81	0	0	0	777.4	134.3	0	0
20	COOH	315.3	1264	62.32	268.2	-151	1020	-66.17	0	-297.8	0	-256.3	312.5	-338.5	0	0	0	0	-313.5	0	0

In the liquid phase synthesis of methyl acetate from methyl alcohol and acetic acid, the subgroups of the relevant species are as follows.

Methyl alcohol	:	1 CH$_3$OH
Acetic acid	:	1 CH$_3$, 1 COOH
Methyl acetate	:	1 CH$_3$, 1 CH$_3$COO
Water	:	1 H$_2$O

The parameters used in the UNIFAC calculation for this system are summarized in Table B.3 and Table B.4.

TABLE B.3: UNIFAC-VLE subgroup parameters (for synthesis of methyl acetate system)[†]

Main Group	Subgroup	Group Name	R_k	Q_k
1	1	CH$_3$	0.9011	0.848
6	16	CH$_3$OH	1.4311	1.432
7	17	H$_2$O	0.9200	1.400
11	22	CH$_3$COO	1.9031	1.728
20	43	COOH	1.3013	1.224

TABLE B.4: UNIFAC-VLE interaction parameters, a_{mk}, in kelvins (for synthesis of methyl acetate system)[†]

a_{mk}	k	1	6	7	11	20
m	Name	CH$_2$	CH$_3$OH	H$_2$O	CCOO	COOH
1	CH$_2$	0	697.2	1318	232.1	663.5
6	CH$_3$OH	16.51	0	-181	-10.72	-289.5
7	H$_2$O	300	289.6	0	72.87	-14.09
11	CCOO	114.8	249.6	200.8	0	660.2
20	COOH	315.3	1020	-66.17	-256.3	0

† Adapted from XLUNIFAC Version 1.0

APPENDIX C

CALIBRATION CURVE

This appendix shows the calibration curves for calculation of composition of reagents in the reaction mixture from experiment of the synthesis of methyl acetate from methyl alcohol and acetic acid in a pervaporation membrane reactor. The curves show the contents of reagent in y-axis and area reported by gas chromatography in x-axis.
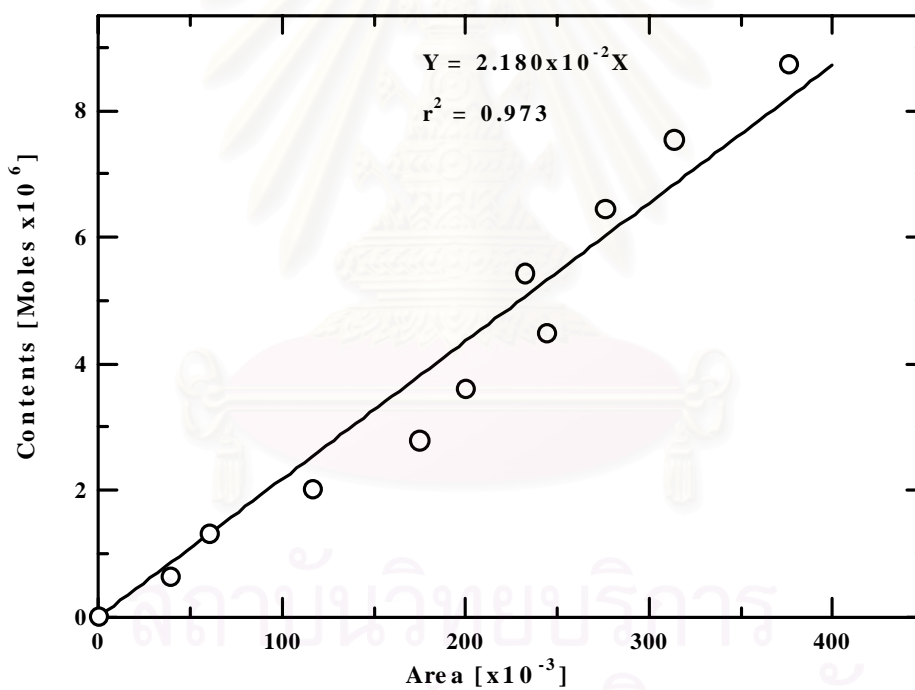

$$Y = 2.180 \times 10^{-2} X$$

$$r^2 = 0.973$$

Figure C.1 Calibration curve of acetic acid
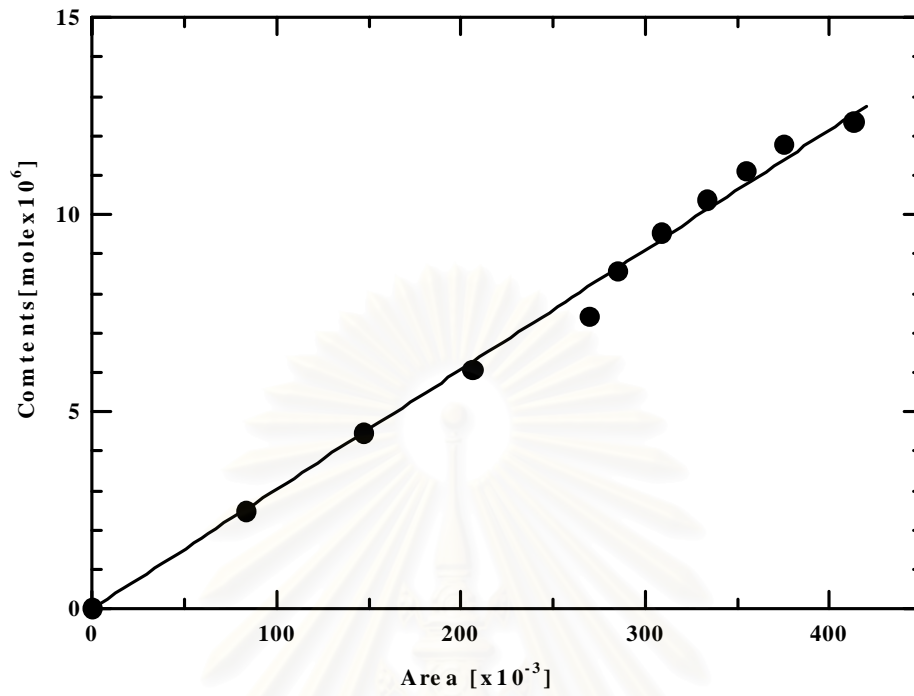
Figure C.2 Calibration curve of methyl alcohol

$Y = 1.839970x10^{-2}$
$r^2 = 0.9894585$
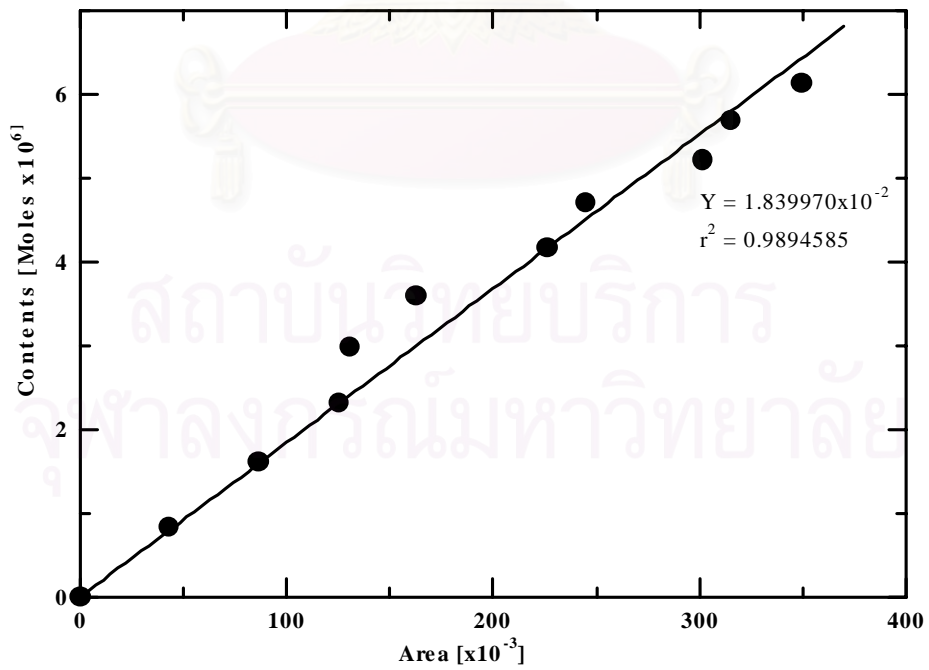
Figure C.3 Calibration curve of methyl acetate
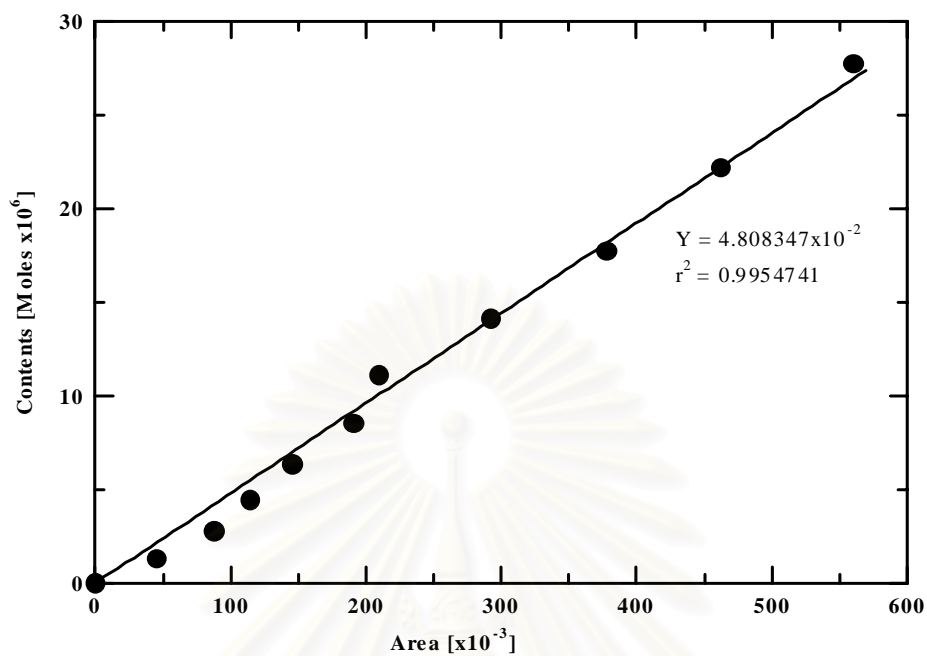
Figure C.4 Calibration curve of water

The calculation of amounts of reagents for the 0.5 µl sample of reaction mixture are shown in Table C.1.

TABLE C.1 Calculation of amount of reagents

Reagent	Area	Amounts (mole)
Water	19828	9.53×10^{-7}
Methanol	237556	7.21×10^{-6}
Acetic acid	87569	4.58×10^{-7}
Methyl acetate	24894	1.91×10^{-6}

APPENDIX D

LIST OF PUBLICATION

1. Assabumrungrat, S., J. Phongpatthanapanich, P. Praserthdam, T. Tagawa, and S. Goto (2003). Theoretical study on the synthesis of methyl acetate from methanol and acetic acid in pervaporation membrane reactors: Effect of continuous flow modes. Chemical Engineering Journal 95: 57-65.

ELSEVIER

Theoretical study on the synthesis of methyl acetate from methanol and acetic acid in pervaporation membrane reactors: effect of continuous-flow modes

Suttichai Assabumrungrat [a,*], Jitkarun Phongpatthanapanich [a],
Piyasan Praserthdam [a], Tomohiko Tagawa [b], Shigeo Goto [b]

[a] *Department of Chemical Engineering, Research Center on Catalysis and Catalytic Reaction Engineering, Chulalongkorn University, Bangkok 10330, Thailand*
[b] *Department of Chemical Engineering, Nagoya University, Chikusa, Nagoya 464-8603, Japan*

Abstract

The synthesis of methyl acetate (MeOAc) from methanol (MeOH) and acetic acid (HOAc) in pervaporation membrane reactors (PVMRs) is discussed in this paper. Three modes of PVMR operation, i.e. semi-batch (SB-PVMR), plug-flow (PF-PVMR) and continuous stirred tank (CS-PVMR) were modeled using the kinetic parameters of the reaction over Amberlyst-15 and permeation parameters for a polyvinyl alcohol (PVA membrane). Both of the reaction and permeation rates are expressed in terms of activities. The PVA membrane shows high separation factors for HOAc and MeOAc but very low for MeOH. The simulation results of SB-PVMR mode show quite good agreement with the experimental results. The study focused on comparing PVMR performances between two modes of continuous-flow operation for various dimensionless parameters, such as Damkohler number (Da), the rate ratio (δ), the feed composition and the membrane selectivity. Flow characteristic within the reactors arisen from different operation modes affects the reactor performance through its influences on the reaction and permeation rates along the reactor. There are only some ranges of operating conditions where CS-PVMR is superior to PF-PVMR.
© 2003 Elsevier Science B.V. All rights reserved.

Keywords: Pervaporation membrane reactor; Methyl acetate synthesis; Activity coefficient; Simulation; Continuous operation

1. Introduction

In recent years, multifunctional reactors have attracted growing interest in both industrial and academic sectors. A number of reactors such as reactive distillation column, membrane reactor, pressure swing reactor and extractive reactor have been proposed to assist conversions of many chemical and biochemical reactions.

For esterification reactions which usually suffer from chemical equilibrium, most investigators have focused on applications of reactive distillation and membrane reactor. Pervaporation membrane reactor (PVMR) as one type of the membrane reactors combines chemical reaction and separation by pervaporation in a single unit. In the pervaporation,

one or more products (usually water) in a reaction liquid mixture contacting on one side of a membrane permeate preferentially through the membrane and the permeated stream is removed as a vapor from the other side of the membrane. As a result, the forward reaction can be enhanced. There are a number of reviews on pervaporation processes [1] and pervaporation combined with distillation and with chemical reactors [2,3]. Advantages of the PVMR are as follows: (a) the simultaneous removal of a product from the reactor enhances the conversion; (b) undesired side reactions can be suppressed; (c) the high conversion is possible at almost stoichiometric feed flow rates and (d) the heat of reaction can be used for separation. Therefore, lower capital investment, lower energy consumption and higher product yields make the pervaporation membrane reactor an interesting alternative to conventional processes.

PVMRs have been implemented in many reaction systems. Zhu et al. [4] studied the esterification reaction of acetic acid (HOAc) with ethanol both by experiment

---

Nomenclature

a_i	activity of species i
a_i'	modified activity of species i ($=K_i a_i/M_i$) (mol/kg)
A	membrane area (m^2)
Da	Damkohler number ($=k_1 W/F_{HOAc,0}$)
E_a	activation energy (J/mol)
F_i	molar flow rate of species i in the reaction side (mol/s)
$\overline{F}_i$	dimensionless molar flow rate of species i in the reaction side ($=F_i/F_{HOAc,0}$)
k_1	reaction rate constant (mol/(kg s))
K_e	equilibrium constant
K_i	adsorption parameter of species i
M_i	molecular weight of species i (kg/mol)
N_i	number of mole of species i in the reactor (mol)
P_i	permeability coefficient of species i (mol/(m^2 s))
Q_i	molar flow rate of species i in the permeate side (mol/s)
$\overline{Q}_i$	dimensionless molar flow rate of species i in the permeate side ($=Q_i/F_{HOAc,0}$)
r	reaction rate (mol/(kg s))
R_g	gas constant ($=8.314$ J/(mol K))
t	reaction time (s)
T	operating temperature (K)
W	catalyst weight (kg)
X_{eq}	equilibrium conversion
X_{HOAc}	conversion based on acetic acid

Greeks letters

α_i	separation factor of species i ($=P_{H_2O}/P_i$)
δ	rate ratio ($=P_{H_2O}A/k_1 W$)
ν_i	stoichiometric coefficient
υ	dimensionless axial coordinate
ξ	factor multiplying with the separation factors at $T = 323$ K

Subscript

0	initial value at $t = 0$

and simulation in a continuous-flow PVMR using a polymeric/ceramic composite membrane. Waldburger and Widmer [2] studied the same reaction in a continuous tube membrane (PVA) reactor. For the pervaporation-assisted process, a decrease of the energy input of over 75% and of the investment and operating costs of over 50% was estimated from the comparison of a conventional distillation process. Feng and Huang [5] studied an esterification reaction in a PVMR operated in the semi-batch mode and found that membrane permeability, membrane area and the volume

of the reaction mixtures are important operating parameters influencing the reactor behavior. Bagnell et al. [6] employed nafion tubes that function both as a reaction catalyst and a pervaporation membrane for the esterification of acetic acid with methanol (MeOH) and *n*-butanol. In the methanol reaction, the yield of methyl acetate (MeOAc) was increased from the usual equilibrium value of 73–77%. In the *n*-butanol reaction, the yield of *n*-butyl acetate increased from 70 to 95%. Okamoto et al. [7] studied the esterification of oleic acid with ethanol in the presence of *p*-toluenesulfonic acid using asymmetric polyimide membranes by simulation. The influence of operating parameters on the reaction time required for a conversion of 98% and on the productivity was investigated. Tanaka et al. [8] applied zeolite membranes to the esterification of acetic acid with ethanol. The studies were carried out by both experiment and simulation using a simple model based on the assumptions that the reaction obeyed second-order kinetics and the permeation flux of each component was proportional to its concentration. The influence of operating parameters on variation in conversion with reaction time was investigated by means of the simulation using the model. Liu and co-workers [9,10] studied on the esterification of acetic acid with *n*-butanol catalyzed by Zr(SO$_4$)·4H$_2$O using cross-linked polyvinyl alcohol (PVA) membranes. Experiments and simulations were conducted to investigate the effects of several operating parameters, such as reaction temperature, initial molar ratio of acetic acid to *n*-butanol, ratio of the membrane area to the reacting mixture volume and catalyst concentration, on the PVMR. Domingues et al. [11] studied kinetics and equilibrium shift of a discontinuous esterification of benzyl alcohol with acetic acid using a commercial GFT membrane. A theoretical model was developed and the simulation results agreed well with the obtained experimental results. Xuehui and Lefu [12] modeled a semi-batch esterification process coupled by pervaporation and established a new method for measuring model parameters. Our previous work considered the synthesis of ETBE from TBA and EtOH in PVMR operated in the semi-batch mode [13].

It should be noted that a model of a plug-flow pervaporation membrane reactor has already been included in a recent book [14]. The same author also extended their modeling works to include other configurations such as continuously stirred, batch, recycle plug-flow, recycle continuously stirred and recycle batch pervaporation membrane reactors [15].

In this paper, the synthesis of methyl acetate from methanol and acetic acid is used as a reaction example for comparing the performances of PVMRs operated in plug-flow (PF-PVMR) and continuous stirred tank (CS-PVMR) modes. Mathematical models using kinetic parameters of the reaction over Amberlyst-15 and permeation data for a polyvinyl alcohol membrane are developed and effects of various operating parameters expressed as dimensionless groups are investigated.

2. Mathematical modeling

2.1. Kinetics of the reaction

The reaction taking place in the reactor can be summarized as follows:
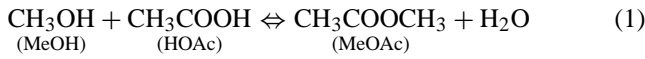
$$CH_3OH + CH_3COOH \Leftrightarrow CH_3COOCH_3 + H_2O \quad (1)$$
$$\text{(MeOH)} \qquad \text{(HOAc)} \qquad \text{(MeOAc)}$$

The rate model and the kinetic parameters of the reaction over Amberlyst-15 are expressed as follows [16]:

$$r = \frac{k_1(a'_{HOAc}a'_{MeOH} - a'_{MeOAc}a'_{H_2O}/K_e)}{(a'_{HOAc} + a'_{MeOH} + a'_{MeOAc} + a'_{H_2O})^2}; \quad \text{with}$$

$$a'_i = \frac{K_i a_i}{M_i}, \quad k_1 = 8.497 \times 10^9 \exp\left(\frac{-60470}{R_g T}\right),$$

$$K_e = 7.211 \times 10^{-2} \exp\left(\frac{3260}{R_g T}\right) \quad (2)$$

and $K_{HOAc} = 3.15$, $K_{MeOH} = 5.64$, $K_{MeOAc} = 4.15$, $K_{H_2O} = 5.24$.

The activity (a_i) can be calculated using the UNIFAC method.

2.2. Rates of pervaporation

Assuming that partial pressure of all species in the permeate side was low, the permeation rate of species i through the membrane can be expressed as

$$Q_i = AP_i a_i \quad (3)$$

The relationship between the permeability coefficient and operating temperature can be correlated by the Arrhenius equation.

$$P_i = P_{i,0} \exp\left(\frac{-E_a}{R_g T}\right) \quad (4)$$

2.3. Modeling of pervaporation membrane reactors

Three operation modes of PVMRs, i.e. semi-batch (SB-PVMR), continuous stirred tank (CS-PVMR) and plug-flow (PF-PVMR) were considered in the study. The mathematical models were obtained from material balances around the reactors, assuming the reactors behaved ideally. In addition, isothermality, negligible pressure drop, negligible heat- and mass-transfer resistances aside from the permeation process and no coupling effect of mixtures on the permeability were assumed. The sets of equations for different operating modes can be summarized as follows:

$$\frac{d}{dt} N_i = v_i W k_1 \frac{a'_{HOAc}a'_{MeOH} - a'_{MeOAc}a'_{H_2O}/K_e}{(a'_{HOAc} + a'_{MeOH} + a'_{MeOAc} + a'_{H_2O})^2}$$
$$- AP_i a_i \quad \text{(SB-PVMR)} \quad (5)$$

$$\frac{d}{dv} \overline{F}_i = v_i Da \frac{a'_{HOAc}a'_{MeOH} - a'_{MeOAc}a'_{H_2O}/K_e}{(a'_{HOAc} + a'_{MeOH} + a'_{MeOAc} + a'_{H_2O})^2}$$
$$- \frac{Da\,\delta a_i}{\alpha_i} \quad \text{(PF-PVMR)} \quad (6)$$

$$\frac{d}{dv} \overline{Q}_i = \frac{Da\,\delta a_i}{\alpha_i} \quad \text{(PF-PVMR)} \quad (7)$$

$$\overline{F}_{i,0} - \overline{F}_i + v_i Da \frac{a'_{HOAc}a'_{MeOH} - a'_{MeOAc}a'_{H_2O}/K_e}{(a'_{HOAc} + a'_{MeOH} + aa'_{MeOAc} + a'_{H_2O})^2}$$
$$- \frac{Da\,\delta a_i}{\alpha_i} = 0 \quad \text{(CS-PVMR)} \quad (8)$$

Various design operating parameters and physical property parameters are characterized in dimensionless groups to facilitate parametric analysis for the comparison of reactor performances under different operation modes.

(1) Damkohler number, Da ($=k_1 W/F_{HOAc,0}$) is a measure of the residence time.
(2) The rate ratio, δ ($=P_{H_2O}A/k_1 W$) is a measure of the ratio between permeation rate and reaction rate.
(3) The separation factor, α_i ($=P_{H_2O}/P_i$) is a measure of membrane selectivity.

Some of the above assumptions may not be valid in all ranges of operating conditions of the PVMRs. Coupling effects in liquid mixtures are known to have a significant impact on actual permeabilities. For PF-PVMR, the axial pressure drop can be significant at high Reynolds numbers and the mass-transfer resistance between the liquid bulk and the surface of catalyst particles and also of the membrane surface becomes significant at large value of Da. In addition, non-ideal conditions such as complete mixing in CS-PVMR; non-isothermal condition; radial and axial gradient of concentration and temperature, should exist in actual operation of both modes. More rigorous models should be investigated in future studies.

EQUATRAN-G (all-purpose equation solver, Omega Simulation Co. Ltd.) was employed to solve the equations.

Comparison between our models and models of Lim et al. [15] reveals that despite of different dimensionless terms, the models are based on the same fundamental. The models take into account the non-ideal effect by expressing the reaction and permeation rates in terms of the activities. The reactor is assumed to behave as an ideal reactor and the concentration polarization effect is considered negligible. In addition, the membrane is assumed to be completely unreactive.

However, our models are based on the experimental data of reaction rates and permeation rates.

3. Experimental

3.1. Materials

PVA membranes (PERVAP 2201) supplied by Sulzur Chemtech GmbH-Membrane Systems and Amberlyst-15
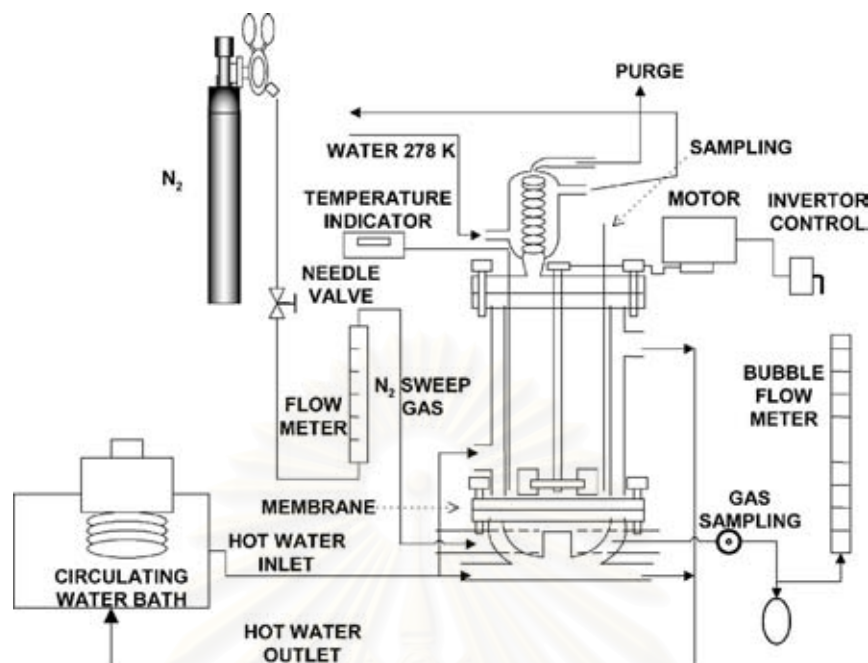
Fig. 1. Experimental apparatus.

obtained from Fluka were used as a water-selective membrane and a catalyst, respectively. Analytic grade methanol (MeOH) and acetic acid (HOAc) were used in the study.

3.2. Permeation study

Fig. 1 shows a schematic diagram of the permeation measurement apparatus. The PVA membrane with an effective area of $63 \, \text{cm}^2$ was placed between two chambers. Hot water was circulated in jackets around the chambers to keep the system at a constant temperature. A disk turbine fully stirred a liquid mixture in the upper chamber while a condenser was attached to the system to condense all vapors leaving the reaction chamber. N_2 sweep gas at a constant molar flow rate of 8.9×10^{-5} mol/s was fed to the permeation side in the lower chamber to increase the driving force of the permeation. The molar flux of each species was obtained by measuring the exit volume flow rate and its composition by a bubble flow meter and a gas chromatography with a Gaskuropack 54 packed column, respectively. It should be noted that the concentration change in the liquid mixture could be neglected due to small amount of permeation compared to the amount of the liquid mixture.

3.3. Pervaporation membrane reactor studies

Experiments on the semi-batch pervaporation membrane reactor were carried out in the same apparatus for the permeation study; however, a frame of four catalyst baskets (as shown in Fig. 2) was mounted on the rotating shaft. The cylindrical baskets (i.d. = 2.5 cm and length = 6 cm) were

made of stainless steel screens. The catalyst, Amberlyst-15 (average diameter = 0.78 mm) was packed into the basket. The frame was held above the liquid level by upper hooks as shown in Fig. 2(a). After the nitrogen flow rate and temperature were maintained at desired values, the reaction was
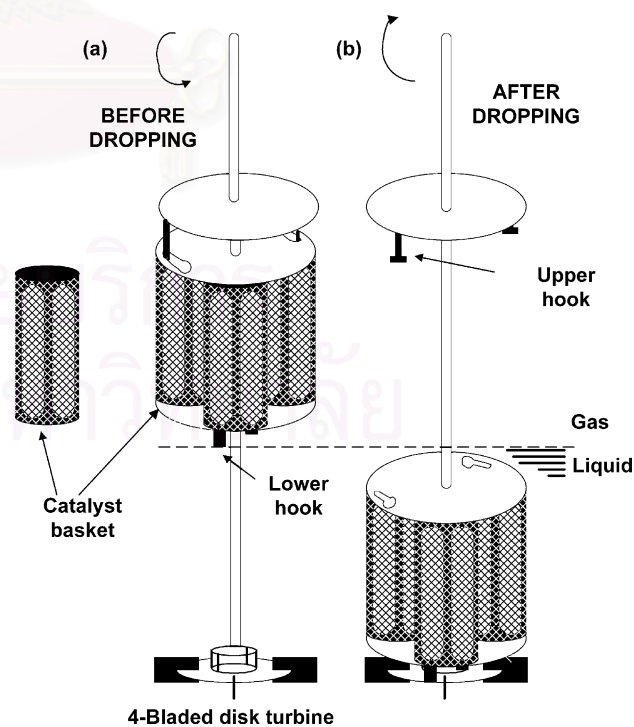

Fig. 2. Details of catalyst basket assembly: (a) before dropping and (b) after dropping.

started by changing the direction of agitation so that the frame of baskets dropped into the liquid mixture and, hence, an accurate start-up time can be determined [17]. The lower hooks were securely connected with slots on the disk turbine and the frame was rotated without slip as shown in Fig. 2(b). The stirring speed was fixed at the highest speed of 1210 rpm to reduce external mass-transfer resistance.

4. Results and discussion

4.1. Permeation studies

Table 1 summarizes the liquid mole fraction, liquid activity, permeability coefficients and separation factors for the permeation experiments of quaternary mixtures (H_2O–MeOH–HOAc–MeOAc) at three temperature levels. It was found that the permeation of acetic acid is negligibly small whereas methanol can permeate through the membrane at significant rate and, hence, the separation factor of methanol, α_{MeOH}, was low. Increasing the temperature results in the decrease of the separation factors. This behavior is observed in many other systems [18]. It should be noted that the expressions shown in terms of activity are more appropriate as the activity deviates significantly from ideality. The obtained permeability coefficients were fitted with good agreement with the Arrhenius equation (shown in Fig. 3) and the expressions are as follows:

$$P_{H_2O} = 2.01 \times 10^1 \exp\left(\frac{-3173}{T}\right) \tag{9}$$

$$P_{MeOH} = 2.92 \times 10^5 \exp\left(\frac{-6756}{T}\right) \tag{10}$$

$$P_{MeOAc} = 7.88 \times 10^7 \exp\left(\frac{-9385}{T}\right) \tag{11}$$
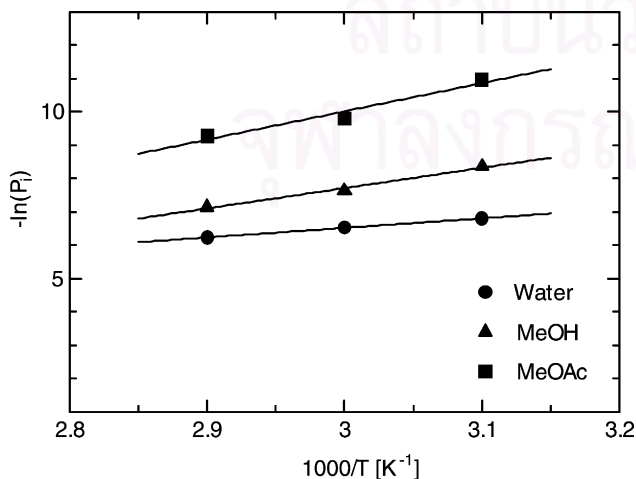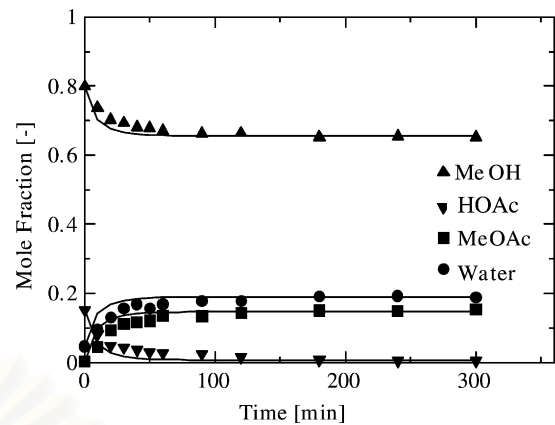

Fig. 3. Arrhenius plot of permeability.

Fig. 4. Comparison between experimental and simulation results of SB-PVMR.

4.2. Pervaporation membrane reactor studies

Fig. 4 compares the experimental and simulation results of SB-PVMR. The initial moles of HOAc and MeOH were 1 and 5 mol, respectively, and the operating temperature was at $T = 333$ K. The model predicts the experimental results quite well. Discrepancy may be arisen from the deviation of permeability coefficients with compositions due to the interaction between components or from non-ideal behavior in the reactor. However, to simplify the model, this effect was neglected in the study.

4.3. Comparison between two modes of continuous operation

4.3.1. Effect of Damkohler number (Da)

Fig. 5 shows the effect of the Damkohler number (Da) on conversion (X_{HOAc}) at various values of the rate ratio (δ). The simulations were based on the values of separation factors (α_i) at $T = 323$ K and the stoichiometric feed ratio. The conversion (X_{HOAc}) is defined as follows:

$$X_{HOAc} = 1 - \frac{\overline{F}_{HOAc} + \overline{Q}_{HOAc}}{\overline{F}_{HOAc,0}}$$

Increasing the values of Damkohler number (Da) increases residence time and, hence, higher conversions are achieved in both PF-PVMR and CS-PVMR modes. The rate ratio (δ) plays an important role on the performance of PVMR. The case with δ = 0 represents conventional reactors whose maximum conversion is limited at an equilibrium value. At higher value of δ, it is possible to exceed the equilibrium conversion encountered in the conventional reactors. This is in agreement with experimental observations in other systems [4,19]. Comparing between two operation modes, it is found that PF-PVMR offers higher conversions than CS-PVMR.

4.3.2. Effect of rate ratio (δ)

Fig. 6 shows the effect of the rate ratio (δ) at 4 values of Damkohler number (Da = 0.5, 1, 25 and 75). There exists

Table 1
Feed composition, feed activity, permeability coefficients and separation factor at three temperature levels

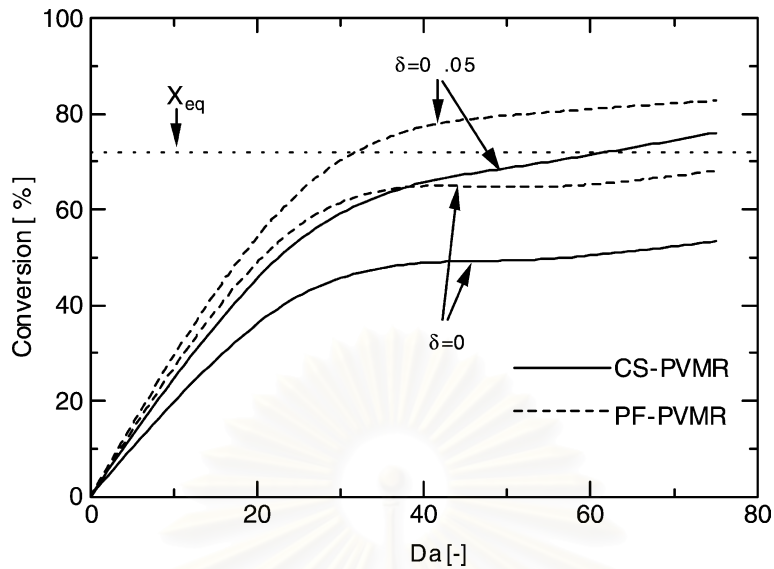| Temperature (K)	Liquid mole fraction				Liquid activity				Permeability coefficient (mol/(m^2 s))				Separation factor			
	Water	MeOH	MeOAc	HOAc	Water	MeOH	MeOAc	HOAc	Water	MeOH	MeOAc	HOAc	Water	MeOH	MeOAc	HOAc
323	0.1009	0.6748	0.0461	0.1782	0.1720	0.6724	0.0877	0.1672	1.11×10^{-3}	2.33×10^{-4}	1.73×10^{-5}	0	1.0	4.7	64	∞
333	0.1127	0.6617	0.0513	0.1743	0.1916	0.6612	0.0976	0.1670	1.45×10^{-3}	4.79×10^{-4}	5.49×10^{-5}	0	1.0	3.0	26	∞
343	0.1201	0.6378	0.0616	0.1804	0.2055	0.6396	0.1144	0.1758	1.96×10^{-3}	7.88×10^{-4}	9.35×10^{-5}	0	1.0	2.5	21	∞

Fig. 5. Effect of Damkohler number (*Da*) on conversion.

an optimum rate ratio (δ), which provides a maximum conversion, for each value of Damkohler number (*Da*). Increasing the rate ratio (δ) at its low values is beneficial to the system due to the enhanced forward reaction from the removal of product H_2O; however, the effect of reactant loss retards the improvement at high values of the rate ratio (δ) as shown in Fig. 7 for $Da = 25$. The presence of an optimum rate ratio was observed in another system for ethyl acetate production in both PF-PVMR and CS-PVMR modes [15].

Loss of component in *y*-axis (Fig. 7) represents the value of $\overline{Q_i}/\overline{F}_{HOAc,0}$. The superiority among PF-PVMR and CS-PVMR in term of maximum obtainable conversion was obviously dependent on the value of Damkohler number

(*Da*). At low value, CS-PVMR is superior to PF-PVMR; however, the opposite results are observed at higher values. It should be noted that the results reported by Lim et al. [15] only indicate the range where PF-PVMR shows a superior performance than CS-PVMR.

Differences in reactor performances between two operation modes are arisen mainly from the different flow characteristics within the reactors. In CS-PVMR, due to well-mixed condition, the reactant concentrations are at their lowest values and, consequently, the reaction takes place at its lowest rate. However, when considering the separation point of view, the well-mixed condition may be beneficial to the system. Because the product concentrations
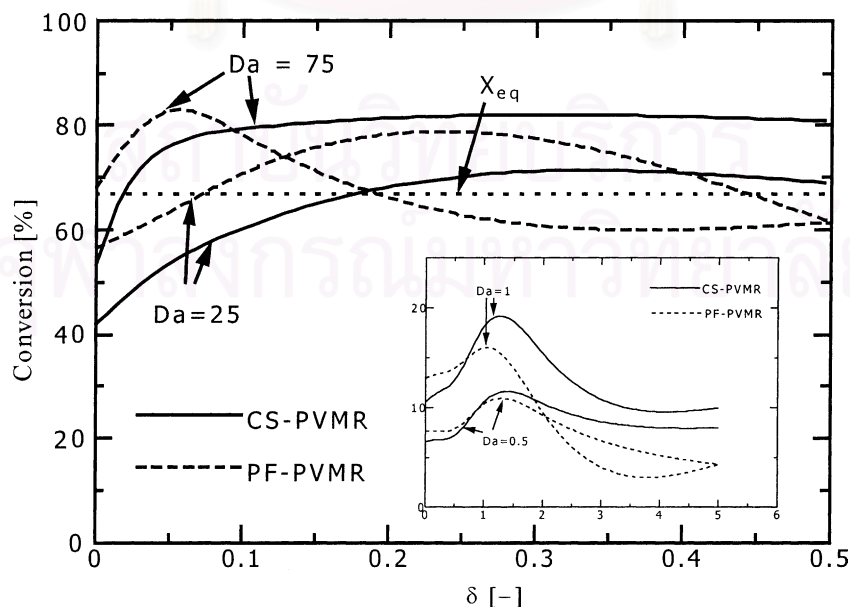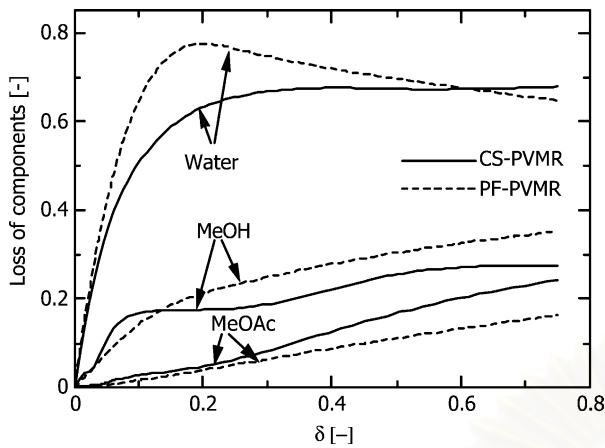

Fig. 6. Effect of rate ratio (δ) on conversion.

Fig. 7. Effect of rate ratio (δ) on reactant/product losses for $Da = 25$.

especially H_2O and the reactant concentrations are at their highest and lowest values, respectively, the entire membrane is efficiently utilized for product removal and, in addition, the reactant losses are at the smallest rates. Considering PF-PVMR, the plug-flow condition usually allows the reaction to proceed at higher extent compared to the well-mixed condition due to high reactant concentrations near the reactor entrance; however, it leads to high reactant losses and low product removal at the initial section. In short, the different flow characteristics within the reactors under different operation modes affect the performance of PVMRs via the effects on the rates of reaction and separation.

At low Damkohler number ($Da = 0.5$ and 1), CS-PVMR is superior to PF-PVMR. Because the residence time is small, the reaction proceeds at small extent. The effect of H_2O removal on enhancing forward reaction in CS-PVMR is higher than PF-PVMR due to the efficient utilization

of membrane area. However, at higher Damkohler number (Da), the increasing reaction rate in PF-PVMR predominates. The reaction moves forward at higher extent and the H_2O removal is high near the end of the reactor. As a result, PF-PVMR is superior to CS-PVMR. It is noted that it is desirable to operate the reactor at high conversion so PF-PVMR seems to be a favorable mode in a practical operation. In addition, the optimum rate ratio (δ) of CS-PVMR is always higher than that of PF-PVMR, indicating that CS-PVMR requires higher membrane area than PF-PVMR.

4.3.3. Effect of feed composition

Since MeOH permeates through the membrane at significant rate, it is likely to operate the reactor with feed composition of MeOH higher than the stoichiometic value. Fig. 8 shows the effect of feed composition on the maximum conversion at $Da = 25$ and 75. The maximum conversion was determined by varying the values of the rate ratio (δ) as illustrated in the previous section. It was found that the optimum feed ratio (MeOH/HOAc) is approximately 1.8. Higher feed ratio results in the decreased feed concentration and reaction rate; however, at feed ratio lower than the optimum value the effect of reactant loss limits the conversion.

4.3.4. Effect of membrane selectivity

Fig. 9 shows the effect of membrane selectivity on the conversion for $Da = 25$. ξ is defined as the factor multiplying with the separation factors at $T = 323$ K. It is found that for $\xi = 1$, at high values of the rate ratio (δ) the conversion decreases with the increase of the rate ratio (δ) due to the effect of reactant loss (as shown in Fig. 10). There is no significant improvement when ξ increases from 10 ($\alpha_{MeOH} = 47$) to 100 and 1000 ($\alpha_{MeOH} = 470$ and 4700).
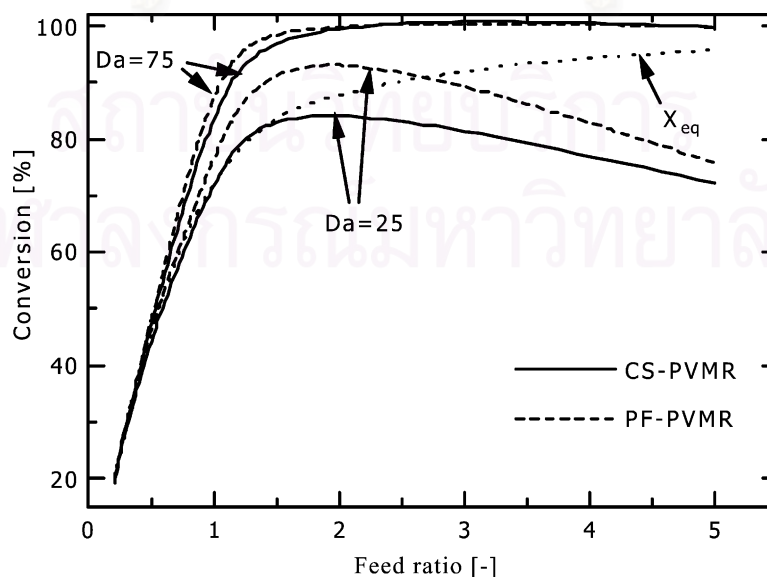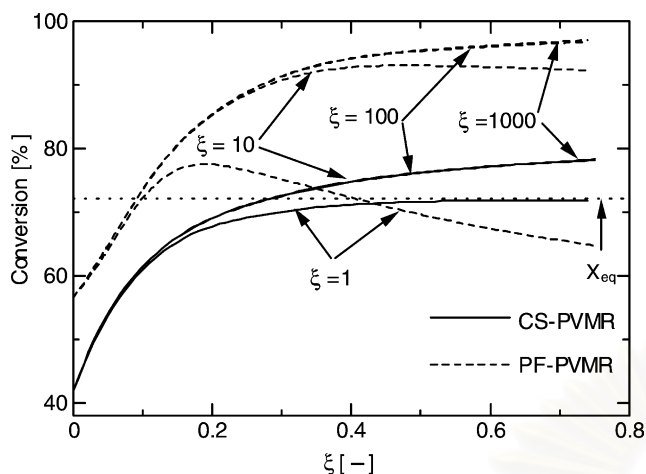

Fig. 8. Effect of feed composition on conversion.

Fig. 9. Effect of membrane selectivity on conversion.

Further simulations of PF-PVMR reveals that at $\delta = 0.75$, membranes with $\alpha_{MeOH} = 47$, 141 and 188 are enough to offer the conversions of 95.0, 98.8 and 99.2%, respectively, of that obtained when $\alpha_{MeOH} = 4700$, indicating that there is a range of membrane selectivity which plays an important role on the reactor performance. Again, it is observed that the maximum obtainable conversion of PF-PVMR is superior to that of CS-PVMR at higher membrane selectivity.

Loss of methanol in y-axis (Fig. 10) represents the value of $\overline{Q}_{MeOH}/\overline{F}_{HOAc,0}$. For $\xi = 1$, at high values of the rate ratio (δ) the loss of methanol in PF-PVMR is higher than that in CS-PVMR. However, at higher ξ (=100, 1000), the loss of methanol becomes negligible. Therefore, the selection of pervaporation membrane with higher separation factor of methanol to water is required.
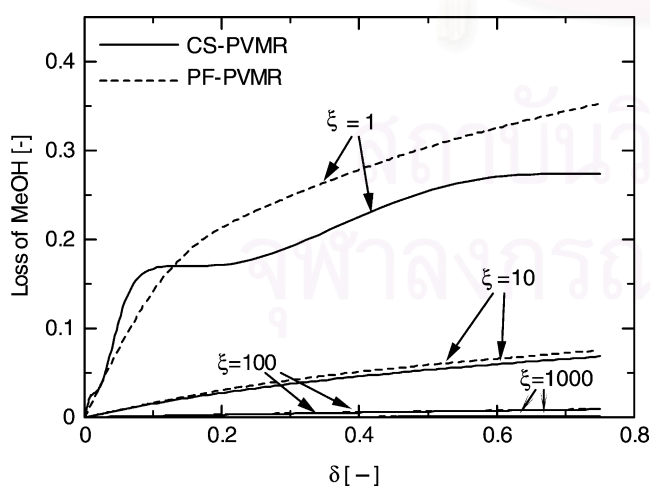

Fig. 10. Effect of membrane selectivity on MeOH loss.

5. Conclusion

Modeling of the esterification of acetic acid with methanol in the pervaporation membrane reactors demonstrates the following:

(a) PF-PVMR is a favorable mode although there are some ranges of operating conditions where CS-PVMR is superior to PF-PVMR.
(b) Flow characteristic in the reactor arisen from different mode affects the reactor performance through its influences on the reaction and permeation rates along the reactor.
(c) A membrane with high selectivity is essential for PVMR to achieve high reactor performance.

Acknowledgements

References

[1] B.K. Dutta, W. Ji, S.K. Sikdar, Sep. Purif. Methods 25 (1996) 131–224.
[2] R.M. Waldburger, F. Widmer, Chem. Eng. Tech. 19 (1996) 117–126.
[3] F. Lipnizki, R.W. Field, P.K. Ten, J. Membr. Sci. 153 (1999) 183–210.
[4] Y. Zhu, R.G. Minet, T.T. Tsotsis, Chem. Eng. Sci. 51 (1996) 4103–4113.
[5] X. Feng, R.Y.M. Huang, Chem. Eng. Sci. 51 (1996) 4673–4679.
[6] L. Bagnell, K. Cavell, A.M. Hodges, M.A.T. Seen, J. Membr. Sci. 85 (1993) 291–299.
[7] K. Okamoto, M. Yamamoto, Y. Otoshi, T. Semoto, M. Yano, K. Tanaka, J. Chem. Eng. Jpn. 26 (1993) 475–481.
[8] K. Tanaka, R. Yoshikawa, C. Ying, H. Kita, K. Okamoto, Catal. Today 67 (2001) 121–125.
[9] Q.L. Liu, Z. Zhang, H.F. Chen, J. Membr. Sci. 182 (2001) 173–181.
[10] Q.L. Liu, H.F. Chen, J. Membr. Sci. 196 (2002) 171–178.
[11] L. Domingues, F. Recasens, M.A. Larrayoz, Chem. Eng. Sci. 54 (1999) 1461–1465.
[12] L. Xuehui, W. Lefu, J. Membr. Sci. 186 (2001) 19–24.
[13] W. Kiatkittipong, S. Assabumrungrat, P. Praserthdam, S. Goto, J. Chem. Eng. Jpn. 35 (2002) 547–556.
[14] J.G.S. Marcano, T.T. Tsotsis, Catalytic Membranes and Membrane Reactors, Wiley, Weinheim, 2002.
[15] S.Y. Lim, B. Park, F. Hung, M. Sahimi, T.T. Tsotsis, Chem. Eng. Sci. 57 (2002) 4933–4946.
[16] T. Popken, L. Gotze, J. Gmehling, Ind. Eng. Chem. Res. 39 (2001) 2601.
[17] S. Ishigaki, S. Goto, J. Chem. Eng. Jpn. 27 (1994) 309–313.
[18] P. Sampranpiboon, R. Jiraratananon, D. Uttapap, X. Feng, R.Y.M. Huang, J. Membr. Sci. 173 (2000) 53–59.
[19] R.M. Waldburger, F. Widmer, W. Heinzelmann, Chem. Eng. Tech. 66 (1994) 850–854.

VITA

Mr. Jitkarun Phongpatthanapanich was born in August 12th, 1979 in Nakhon Sri Thammarat, Thailand. He finished high school from Triam Udom Suksa School, Bangkok in 1998, and received bachelor's degree in Chemical Engineering from the department of Chemical Engineering, Faculty of Engineering, Chulalongkorn University, Bangkok, Thailand in 2002.